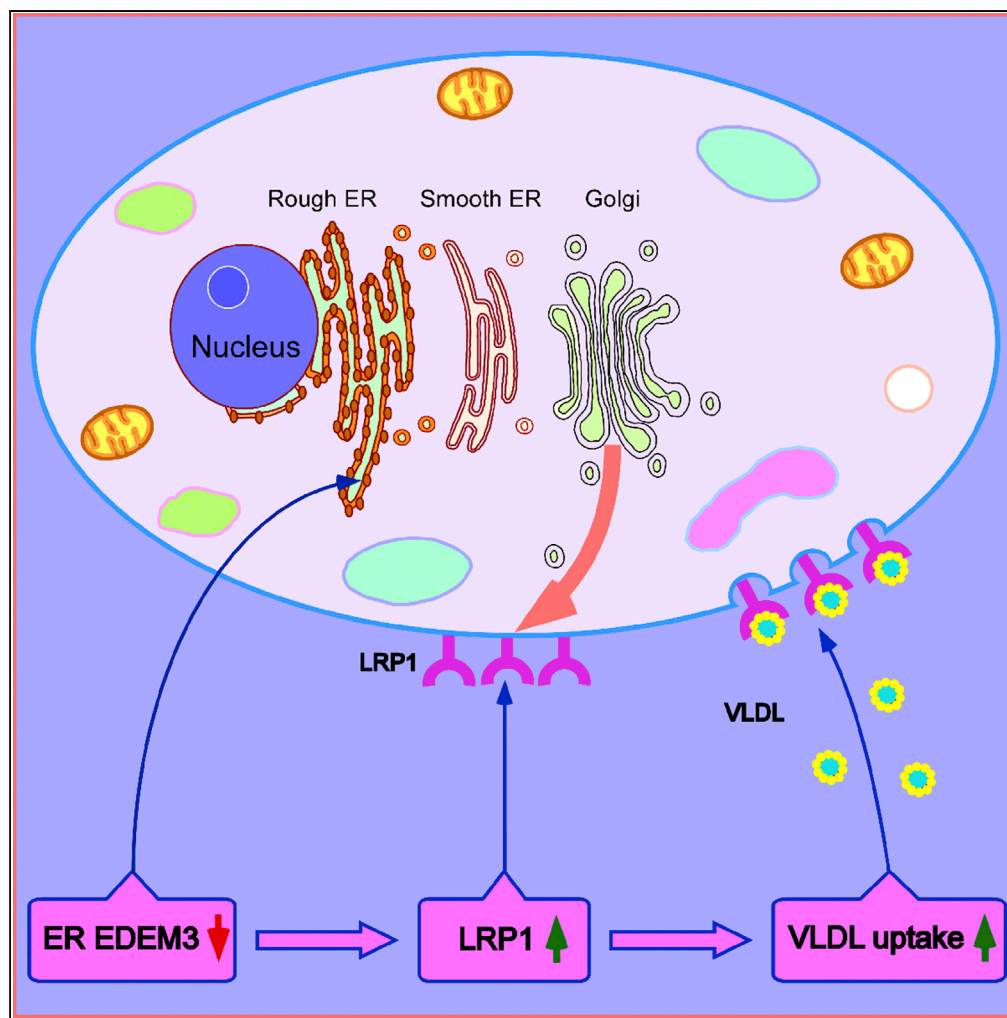


## Article

## EDEM3 Modulates Plasma Triglyceride Level through Its Regulation of LRP1 Expression



Yu-Xin Xu, Gina M. Peloso, Taylor H. Nagai, ..., Clary B. Clish, Daniel Rader, Sekar Kathiresan

yuxin.xu2006@gmail.com,  
yxu19@mit.edu (Y.-X.X.)  
skathiresan1@partners.org  
(S.K.)

**HIGHLIGHTS**

Genetic deficiency of EDEM3 leads to lower blood triglyceride (TG) level

EDEM3 deficiency increases VLDL uptake by up-regulating LRP1 receptor expression

Blood TG changes due to EDEM3 mutation correlate with the TG profile of EDEM3 KO cells

Xu et al., iScience 23, 100973  
April 24, 2020 © 2020 The Author(s).  
<https://doi.org/10.1016/j.isci.2020.100973>

## Article

# EDEM3 Modulates Plasma Triglyceride Level through Its Regulation of LRP1 Expression

Yu-Xin Xu,<sup>1,11,\*</sup> Gina M. Peloso,<sup>2</sup> Taylor H. Nagai,<sup>1</sup> Taiji Mizoguchi,<sup>1</sup> Amy Deik,<sup>3</sup> Kevin Bullock,<sup>3</sup> Honghuang Lin,<sup>4</sup> Kiran Musunuru,<sup>5</sup> Qiong Yang,<sup>2</sup> Ramachandran S. Vasam,<sup>6,7</sup> Robert E. Gerszten,<sup>8</sup> Clary B. Clish,<sup>3</sup> Daniel Rader,<sup>9</sup> and Sekar Kathiresan<sup>1,10,\*</sup>

## SUMMARY

**Human genetics studies have uncovered genetic variants that can be used to guide biological research and prioritize molecular targets for therapeutic intervention for complex diseases. We have identified a missense variant (P746S) in *EDEM3* associated with lower blood triglyceride (TG) levels in >300,000 individuals. Functional analyses in cell and mouse models show that *EDEM3* deficiency strongly increased the uptake of very-low-density lipoprotein and thereby reduced the plasma TG level, as a result of up-regulated expression of LRP1 receptor. We demonstrate that *EDEM3* deletion up-regulated the pathways for RNA and endoplasmic reticulum protein processing and transport, and consequently increased the cell surface mannose-containing glycoproteins, including LRP1. Metabolomics analyses reveal a cellular TG accumulation under *EDEM3* deficiency, a profile consistent with individuals carrying *EDEM3* P746S. Our study identifies *EDEM3* as a regulator of blood TG, and targeted inhibition of *EDEM3* may provide a complementary approach for lowering elevated blood TG concentrations.**

## INTRODUCTION

High blood triglyceride (TG) level is one of the leading risk factors for coronary artery diseases (CADs) (Bauer et al., 2016; Johansen et al., 2011), along with low-density lipoprotein cholesterol (LDL-C). Human genetic studies have suggested that high TG levels causally affect the risk of CADs independent of LDL-C and high-density lipoprotein cholesterol (HDL-C) (Do et al., 2013). In addition, diabetes mellitus and metabolic syndrome are two major risk factors for CADs (Malik et al., 2004). High blood TG level linked to insulin resistance is a phenotype common to these metabolic diseases. Thus, lowering blood TG level could further reduce the incidence of CADs as well as type 2 diabetes and metabolic syndrome, especially in high-risk individuals. Apolipoprotein (Apo) C3 and angiotensin-like 3 (ANGPTL3) are two molecular targets currently under intensive studies for lowering blood TG (Musunuru et al., 2010; Rammes and Gordts, 2018; Xu et al., 2018). The two targets share the common mechanism of inhibition of lipoprotein lipase (LPL) (Larsson et al., 2013; Lee et al., 2009; Ono et al., 2003). Finding other targets independent of LPL could further lower blood TG levels.

Endoplasmic reticulum (ER)-degradation alpha-mannosidase like protein 3 (EDEM3) plays a crucial role in the ER-associated degradation (ERAD) pathway (Eriksson et al., 2004; Hirao et al., 2006; Olivari and Molinari, 2007). Nascent polypeptides emerging in the ER undergo several quality control processes assisted by ER chaperones and folding factors that ensure proper folding and maturation. Misfolded or unassembled proteins are recognized and subject to degradation (Bernasconi and Molinari, 2011; Hebert et al., 2005; Trombetta and Parodi, 2003). The ER-resident EDEM family of proteins is responsible for identifying misfolded proteins, trimming the mannoses of their N-linked glycans, and signaling them for degradation. It was reported that all the EDEM members have mannosidase activity (Hirao et al., 2006; Hosokawa et al., 2010; Shenkman et al., 2018). It is unclear how EDEM3 specifically recognizes the misfolded proteins. Previous findings have indicated that the enzymatic activity of EDEM3 does not necessarily target only misfolded glycoproteins, as it has been shown to stimulate mannose trimming among the total glycoproteins under the condition of EDEM3 overexpression (Hirao et al., 2006). The biological significance of EDEM3 is still unknown.

We provide evidence that EDEM3 may be another TG-lowering target that represents a distinct mechanism in modulating TG metabolism. We identified a rare variant (P746S) in the coding region of EDEM3 using human

<sup>1</sup>Center for Genomic Medicine, Massachusetts General Hospital, Simches 5.500, 185 Cambridge St., Boston, MA 02114, USA

<sup>2</sup>Department of Biostatistics, Boston University School of Public Health, Boston, MA 02118, USA

<sup>3</sup>The Metabolomics Program, Broad Institute, Cambridge, MA 02142, USA

<sup>4</sup>Section of Computational Biomedicine, Department of Medicine, Boston University School of Medicine, Boston, MA 02118, USA

<sup>5</sup>Cardiovascular Institute, Department of Medicine, Perelman School of Medicine, University of Pennsylvania, Philadelphia, PA 19104, USA

<sup>6</sup>Preventive Medicine and Epidemiology, Boston University School of Medicine, Boston, MA 02118, USA

<sup>7</sup>Framingham Heart Study of the NHLBI and Boston University School of Medicine, Framingham, MA 01702, USA

<sup>8</sup>Division of Cardiovascular Medicine, Beth Israel Deaconess Medical Center, Boston, MA 02215, USA

<sup>9</sup>Institute for Translational Medicine and Therapeutics, Perelman School of Medicine, University of Pennsylvania, Philadelphia, PA 19104, USA

<sup>10</sup>Present address: Verve Therapeutics, Cambridge, MA 02142, USA

<sup>11</sup>Lead Contact

\*Correspondence: yuxin.xu2006@gmail.com, yxu19@mit.edu (Y.-X.X.)

Continued



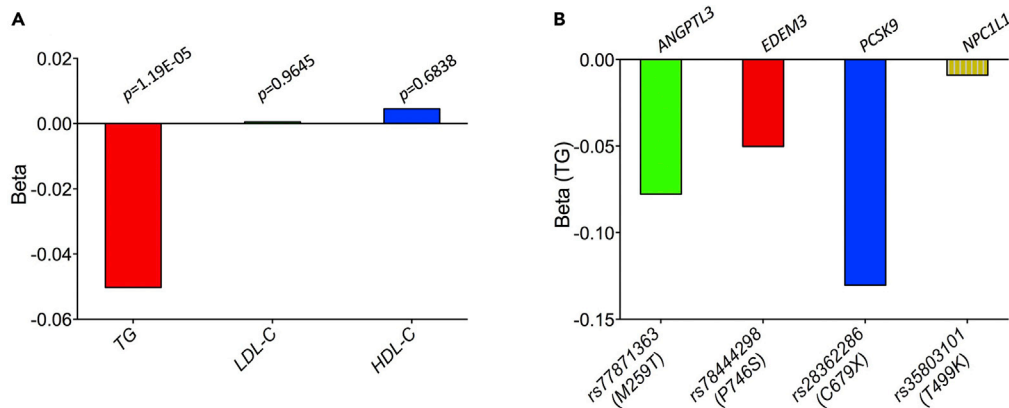


**Figure 1. Genetic Association Study of EDEM3 Missense Mutations with Lipid Phenotypes**

(A) Significant association of EDEM3 SNP rs78444298 (P746S) with blood TG (5% decrease;  $p = 1.2 \times 10^{-5}$ ), but not with LDL-C and HDL-C ( $p > 0.05$ ).

(B) Comparison of the effect of EDEM3 rs78444298 with other missense mutations of TG genes including ANGPTL3 rs77871363, PCSK9 rs28362286 (gain-of-function), and NCP1L1 rs35803101 (negative control) on plasma TG. Beta, which represents the effect size of variant association on  $\log(\text{TG})$ , is displayed in standard deviation units of  $\log(\text{TG})$ .

genetic studies that is specifically associated with lower blood TG. Deletion of EDEM3 gene in two types of human hepatoma HepG2 and Huh7 cells strongly increased the uptake of very-low-density lipoprotein (VLDL) as a result of increased LRP1 expression. Consistent with this observation, knockdown (KD) of hepatic EDEM3 with CRISPR/Cas9 decreased the plasma TG level in mice. Interestingly, we found that EDEM3 gene deletion increased the cell surface mannose presence without increasing the sensitivity of the cells to ER stress, likely due to the compensation by increased RNA processing and ER protein transport, and repressed cellular metabolic processes. Importantly, the cellular lipid metabolite profile under EDEM3 gene deletion largely explains the plasma lipid metabolite results from the individuals carrying the EDEM3 missense variant, P746S. Thus, our findings show that by regulating LRP1 expression, EDEM3 is able to modulate the plasma TG level. Inhibition of EDEM3 expression could offer an alternative path to lower TG levels.

## RESULTS

### A Missense Mutation in EDEM3 Is Linked to Lower Human Plasma TG Levels

To investigate possible roles of EDEM3 in lipoprotein metabolism, we first took a human genetic approach to identify EDEM3 single-nucleotide polymorphisms (SNPs) that might be associated with lipid traits. Common variants near EDEM3 have not been associated with blood TGs in the population (Figure S1) (Willer et al., 2013). We analyzed >300,000 individuals of mainly European ancestry with exome array genotyping available from the Global Lipids Genetics Consortium against plasma lipid levels (Liu et al., 2017). There are many rare variants associated with TG levels (Liu et al., 2017). In the full analysis of exome array variation, we found 142 variants associated with TG levels at an alpha level of 0.0001 and a minor allele frequency less than 5%. Among seven EDEM3 SNPs examined, only one, rs7844298 (P746S), shows statistically significant relations with lower plasma TG level, but not with HDL-C and LDL-C (Table S1 and Figure 1A). Comparing this SNP with other validated missense variants shows that its effect on TG level is ~65% of ANGPTL3 rs77871363 (M259T) and ~38% of PCSK9 rs28362286 (gain-of-function), both of which exhibit the strong link with TG phenotypes (Figure 1B). The SNP is located at the coding region of EDEM3 protease-associated (PA) domain (Figure 2C), which is not present in other EDEM members (Olivari and Molinari, 2007). The SNP's unique domain location and its effect on blood TG concentrations at the population level suggest that EDEM3 may have an unknown mechanism in regulating lipoprotein metabolism.

### Deletion of EDEM3 Gene Strongly Increased VLDL, but Not LDL, Uptake

It is likely that the lower plasma TG level observed in human genetic studies is from the damaging effect of the mutation on the cellular activity of EDEM3. Therefore, to obtain the mechanistic insight of EDEM3 function in lipid metabolism, we tried to delete the gene in human hepatoma cells for functional assays. We used CRISPR/cas9 genome editing system with three single guide RNAs (sgRNAs) that target the exon region of EDEM3 gene

\*Correspondence, Center for Genomic Medicine and Cardiovascular Research Center, Massachusetts General Hospital, Simches 5.252, 185 Cambridge St., Boston, MA 02114, USA: [skathiresan1@partners.org](mailto:skathiresan1@partners.org) (S.K.)

<https://doi.org/10.1016/j.isci.2020.100973>

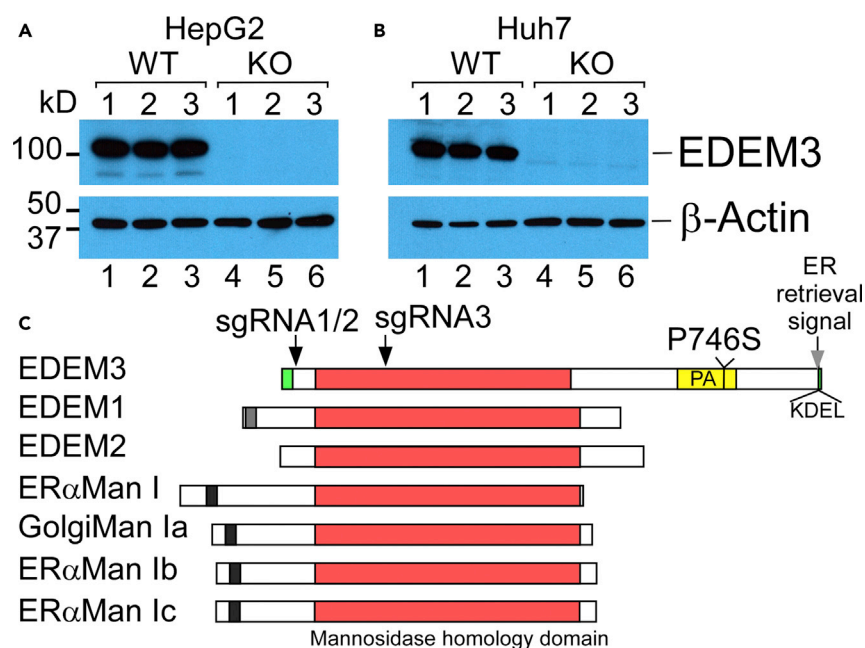


**Figure 2. Confirmation of EDEM3 Gene Deletion in HepG2 and Huh7 Cells**

(A and B) Western analysis of EDEM3 expression. Extracts from EDEM3 WT and KO HepG2 (A) and Huh7 (B) cells were examined with western blotting and probed with anti-EDEM3 and anti- $\beta$ -actin antibodies.

(C) Domain similarity of Class I  $\alpha$ 1,2-mannosidase family members. The conserved mannosidase homology domain, the unique protease-associated (PA) domain, and ER retrieval signal of EDEM3 are highlighted. The positions of sgRNAs and the human EDEM3 P746S mutation are indicated.

(Figure 2B) along with scramble control sgRNAs (Sanjana et al., 2014; Shalem et al., 2014). After screening several hundreds of clones, we obtained EDEM3 knockout (KO) Huh7 and HepG2 cells as well as the scramble controls (wild-type [WT]). Western analysis confirms the deletion of EDEM3 gene specifically in three HepG2 and Huh7 KO clones (Figures 2A and 2B).

The lower TG phenotypes caused by the EDEM3 mutation could be due to enhanced uptake of TG-rich lipoproteins (TGLs), reduced secretion of VLDL, or both. We first tested whether the EDEM3 gene deletion might affect the VLDL uptake. The KO and control Huh7 and HepG2 clones were incubated with human Dil-VLDL (Stephan and Yurachek, 1993). We found that EDEM3 deficiency strongly increased the VLDL uptake in both Huh7 (by 1.6 times) and HepG2 (by  $\sim$ 5.2 times) cells (Figure 3). Dramatic increases were observed in some HepG2 and Huh7 KO clones (by  $\sim$ 2.6 and  $\sim$ 10 times, respectively) (Figures 3A and 3B, bottom images). Similar assays with human Dil-LDL were performed, but no significant changes were observed (Figure S2). Consistent with this, we found that the EDEM3 KO did not significantly change the LDLR expression (Figure S3). The data suggest that deletion of EDEM3 gene increases VLDL, but not LDL, uptake.

### Deletion of EDEM3 Gene Did Not Affect VLDL Secretion

We next investigated whether EDEM3 gene deletion might also affect the VLDL or nascent ApoB secretion. To this end, we carried out time course experiments to monitor nascent ApoB-100 secretion and its accumulation in culture media. Three clones of EDEM3 KO and control HepG2 and Huh7 cells were washed and incubated with fresh media. At various time points, fractions of the media were analyzed with ApoB ELISA. The ApoB in the media reflects the dynamics of ApoB secretion from and uptake into the cells. However, at the earliest time points (i.e., 20 and 40 min), the ApoB in the media most likely represents the nascent ApoB secreted from the cells. We found no significant difference ( $p > 0.05$ ) in the ApoB levels between the KO and control clones in both HepG2 and Huh7 cells at 20 and 40 min time points (Figures 4A and 4B). We then monitored the ApoB concentrations from Huh7 cells for longer period. After 40 min, the ApoB level in the media of Huh7 cells decreased at various time points and became significantly decreased ( $p < 0.05$ ) for all the KO clones at 8 h (Figure 4C). Because EDEM3 gene deletion did not affect the ApoB secretion,

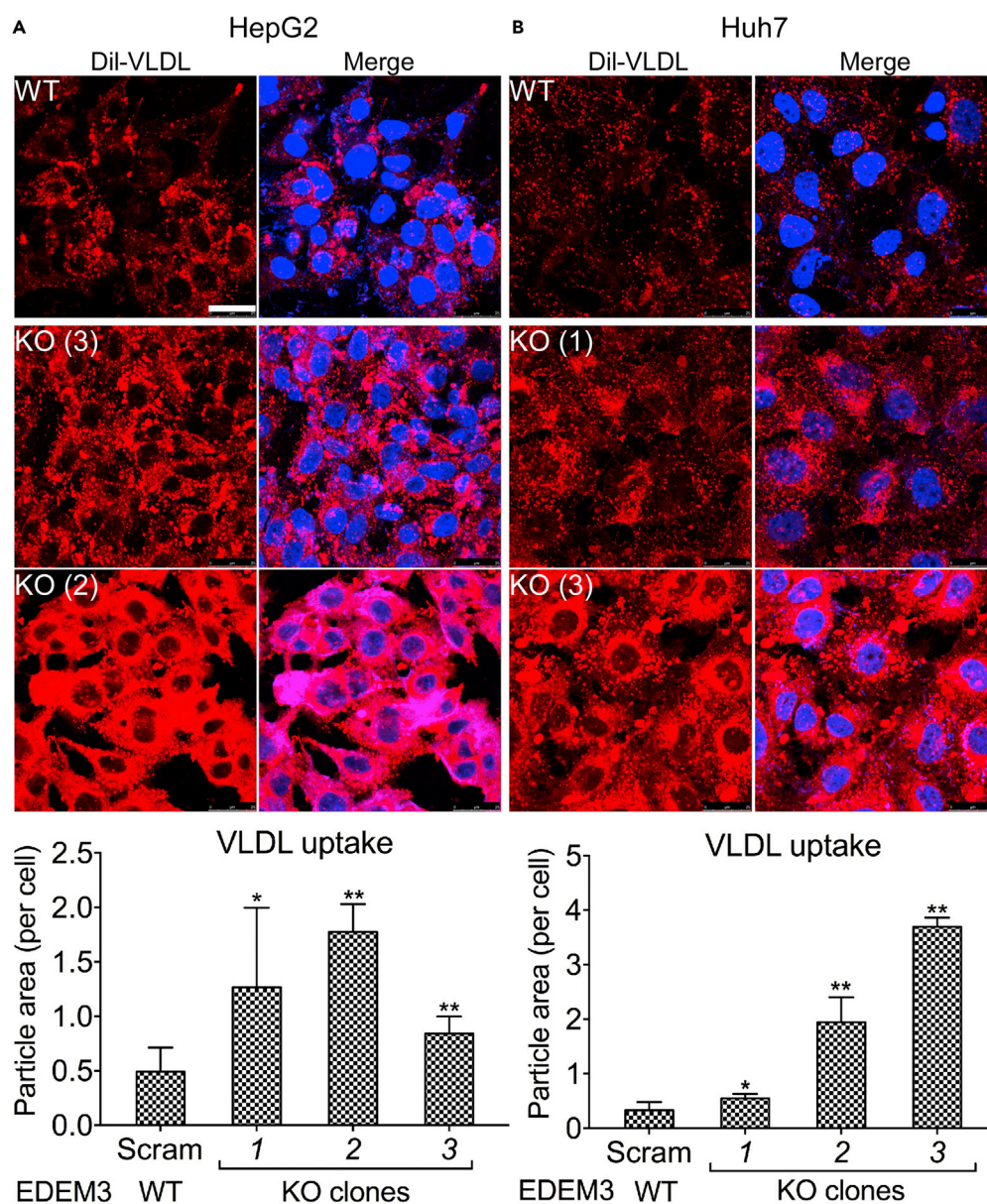


**Figure 3. Deletion of *EDEM3* Gene Strongly Enhanced Dil-VLDL Uptake**

(A and B) (A) Three individual *EDEM3* scramble control (WT) and KO HepG2 (A) and Huh7 (B) clones were incubated with Dil-VLDL. Top, Representative images of the uptake assays from *EDEM3* KO and control cells. Bottom, Quantification of the uptake assays from three clones of the control cells (~200 cells) and KO cells (~500 cells). Cellular Dil-VLDL particle areas were quantified using ImageJ. *p* values (t test) were calculated by comparing the KO cells with the control cells. The error bars represent standard error of the mean (SEM) in the figure. \**p* < 0.05; \*\**p* < 0.01. Scale bar, 25  $\mu$ m.

the increased uptake is most likely responsible for all the decreases of the ApoB in the media. These data are consistent with those from the Dil-VLDL uptake assays, indicating that enhanced VLDL uptake might play a major role in reducing the TG level under *EDEM3* deficiency.

#### Deletion of *EDEM3* Gene Increased LRP1 Expression

In addition to LDLR (Figure S3), there are several other receptors including LRP1 and VLDL receptor (VLDLR) that could be potentially linked to the phenotypes we observed. It should be noted that the expression of VLDLR is low or undetectable in the livers (Nimpf and Schneider, 2000), and most importantly, the VLDLR

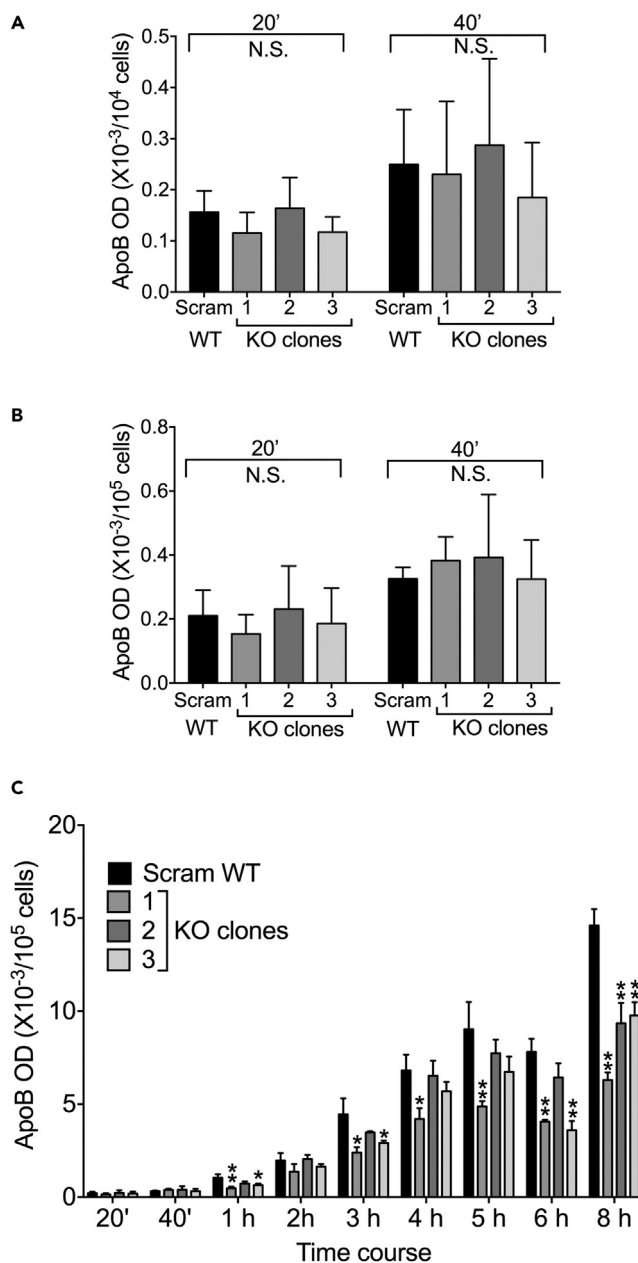


**Figure 4. Deletion of *EDEM3* Gene Reduced ApoB-100 Accumulation in Culture Media without Interfering with Nascent ApoB Secretion**

(A and B) Three individual *EDEM3* scramble control (WT) and KO HepG2 (A) and Huh7 (B) clones were used for time course experiments to monitor ApoB presence in culture media between 20 and 40 min using ApoB ELISA kit.

(C) Complete time course experiment for monitoring culture media ApoB concentrations from Huh7 cells between 20 min and 8 h

p values (t test) were calculated by comparing the KO cells with the control cells. The error bars represent SEM in the figure. \*p < 0.05; \*\*p < 0.01.

KO mice did not display any lipoprotein defects (Frykman et al., 1995). In contrast, hepatic LRP1 was shown to play a central role in clearance of TGLs such as chylomicron and VLDL remnants (Lillis et al., 2008; Rohlmann et al., 1998; Willnow et al., 1994, 1995). Previous study also validated that LRP1 is modified with N-linked glycans (May et al., 2003) and is likely to be the target of *EDEM3* in the ER. It is possible that *EDEM3* modulates the plasma TG level by regulating the LRP1 expression in the livers. To test this

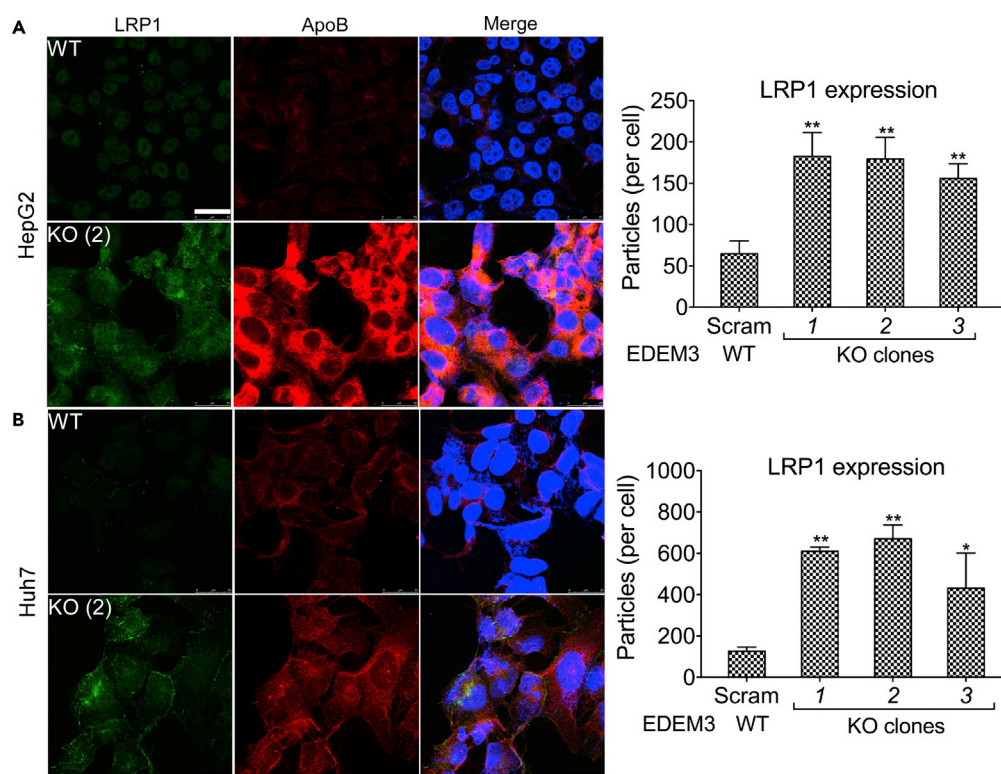


**Figure 5. Deletion of *EDEM3* Gene Increased LRP1 Expression**

(A) Three individual *EDEM3* scramble control (WT) and KO HepG2 (A) and Huh7 (B) clones were stained with anti-LRP1 and anti-ApoB antibodies and analyzed with confocal microscope (left). Images were quantified with ImageJ from 100–200 cells for each clone (right). *p* values (*t* test) were calculated by comparing the results from the KO cells with those from the control cells. The error bars represent SEM in the figure. \**p* < 0.05; \*\**p* < 0.01. Scale bar, 25  $\mu$ m.

hypothesis, we first used indirect immunofluorescence to examine the cell surface LRP1 expression. The *EDEM3* WT and KO HepG2 and Huh7 clones were stained with anti-LRP1 and anti-ApoB antibodies (Xu et al., 2010). The results presented in Figure 5 show that deletion of *EDEM3* gene substantially increased the cell surface LRP1 expression both in HepG2 and Huh7 cells. In the WT control cells, the cell surface LRP1 is barely detectable under the conditions we tested. However, in the KO cells, the LRP1 signal is strongly increased (by ~1.7 times and ~3.5 times increases in HepG2 and Huh7 cells, respectively). The accumulated LRP1 on the cell surface can be clearly seen at the cell peripheries in the flatter KO Huh7 cells (Figure 5B).

We then examined the LRP1 expression with western analysis. Consistent with the above-mentioned immunofluorescence results (Figure 5), it shows that the LRP1 protein level is indeed greatly increased in the *EDEM3* KO HepG2 and Huh7 cells (Figures 6A and 6B). Interestingly, we observed that the LRP1 from the KO cells has slower mobility, which is more obvious from the HepG2 KO cells (Figure 6A, lanes 4–6), indicating that the LRP1 may possess post-translational modification changes related to the activity of *EDEM3* in the ER. Although we detected the increased LRP1 expression, the mobility changes of LRP1 from those of Huh7 KO cells were barely detectable (Figure 6B). It was reported that LRP1 is differentially glycosylated in a tissue-specific manner (May et al., 2003). We reasoned that the LRP1 mobility changes might be related to cell types. Because of mannose hydrolase activity of *EDEM3*, we expected that the LRP1 in the KO cells might retain mannose/glucose, which are supposed to be removed in the ER (Olivari and Molinari, 2007). To test this, the *EDEM3* WT and KO HepG2 clones were stained with fluorescein isothiocyanate-labeled concanavalin A (ConA) (recognizing mannose) and analyzed with flow cytometry. The results show that the KO cells indeed contained stronger signal than the WT cells (Figure 6C). Thus, the data shown here suggest that deletion of *EDEM3* gene increases the cell surface LRP1 expression, which is most likely related to its post-translational processing in the ER.

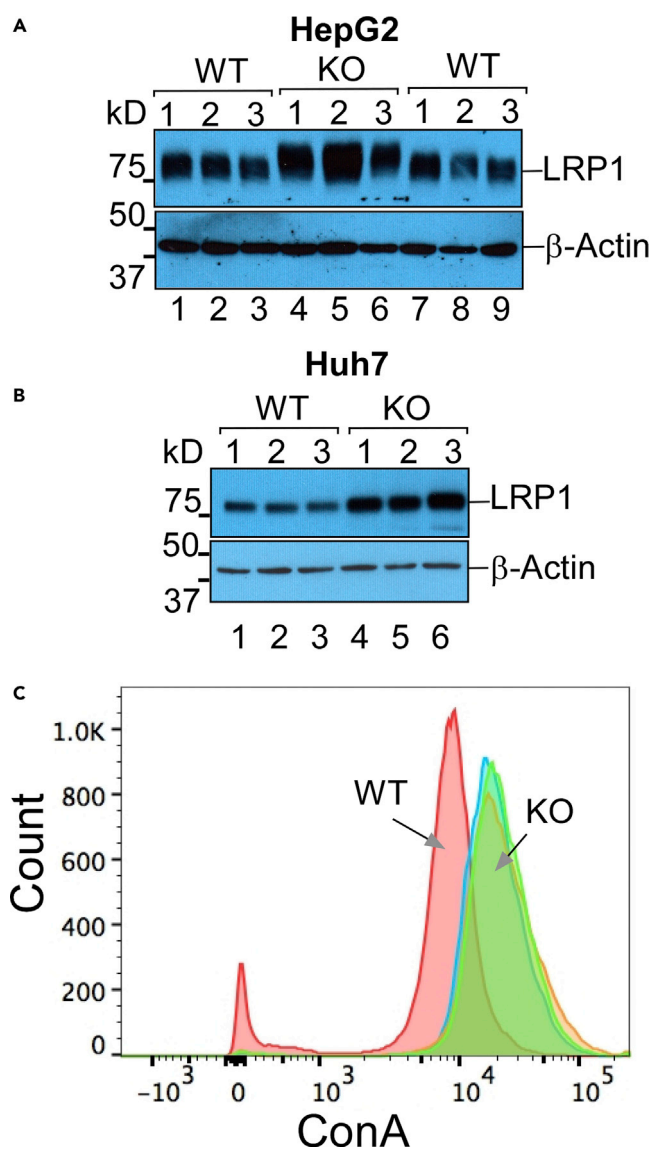


**Figure 6. Deletion of *EDEM3* Gene Increased LRP1 Expression as well as cell Surface Mannose-Containing Proteins**

(A and B) Extracts from three individual *EDEM3* scramble control (WT) and KO HepG2 (A) and Huh7 (B) clones were analyzed with western blotting and probed with anti-LRP1 and anti- $\beta$ -actin antibodies.

(C) The WT and KO HepG2 clones as in (A) were stained with fluorescein isothiocyanate-ConA and fixed with 1% paraformaldehyde. The cells were then analyzed with flow cytometry.

### Complement of *EDEM3* Deletion with WT, but Not P746S Mutant, *EDEM3* Reduced LRP1 Expression and VLDL Uptake

To obtain further functional evidence of *EDEM3* in regulating LRP1 expression and VLDL uptake, we performed complementary analysis of *EDEM3* deletion with WT and P746S mutant *EDEM3*. The *EDEM3* KO HepG2 and Huh7 cells were infected with control lentivirus alone or the lentiviruses harboring the cDNAs of FLAG-tagged WT and P746S mutant *EDEM3*. We focused on the LRP1 from HepG2 cells because it generated more mobility changes (Figure 6A). Western analysis (Figure 7A, middle) confirmed the expression of the WT (Figure 7A, middle, lanes 4–6) and mutant (lanes 7–9) *EDEM3*. The expression of WT *EDEM3* significantly reduced the level of LRP1 (by ~11%). In contrast, the mutant *EDEM3* even increased the LRP1 expression by ~74%. The LRP1 from the KO cells with WT *EDEM3* complement had slightly faster mobility when compared with those from the KO cells and the cells with the mutant *EDEM3* (more obvious for the smaller fragment

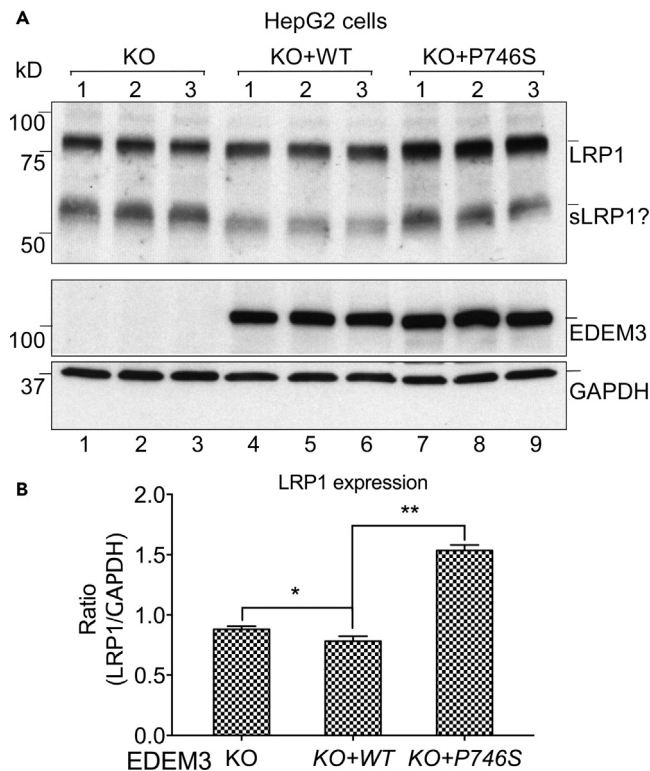


**Figure 7. Complementary Analysis of EDEM3 Gene Deletion with WT and P746S Mutant EDEM3**

(A) EDEM3 KO HepG2 cells were infected with control lentivirus or the same virus containing WT and P746S EDEM3 cDNAs. Extracts from the complementary or control cells were analyzed with western blotting and probed with the antibodies against LRP1, EDEM3, and GAPDH (from top to bottom). sLRP1 is likely a smaller fragment of LRP1.

(B) Normalized quantification of LRP1 expression with GAPDH as in (A). p values (t test) were calculated by comparing the KO + WT cells with the KO or KO + P746S cells.

ANOVA p value < 0.001. The error bars represent SEM in the figure. \*p < 0.05; \*\*p < 0.01.

[sLRP1] of LRP1, compare lanes 4–6 with lanes 3 or 7), indicating modification changes. Immunofluorescence analysis confirmed the LRP1 expression changes in the KO HepG2 cells and the cells with the WT and mutant EDEM3. The increased LRP1 expression correlated with the elevated cellular ApoB signal (Figure S4). Similar results were also obtained from the Huh7 KO with the WT and mutant EDEM3 (Figure S5).

The above-mentioned cells were then used for VLDL uptake assays. The complementary expression of WT EDEM3 drastically reduced the VLDL uptake (by ~62%) when compared with those of the KO HepG2 cells. In contrast, the expression of the mutant EDEM3 in the KO cells increased the VLDL uptake (by nearly two times) when compared with the WT complement (Figure S6). Again, similar results were obtained from Huh7 KO cells and the cells with complementary WT (decreased by ~28%) and mutant (increased by ~57%) EDEM3 expressions (Figure S7). Given the crucial roles of LRP1 in regulating TG metabolism (Lillis et al., 2008), the increased expression levels of LRP1 most likely explain the elevated VLDL uptakes in both cell types. Therefore, the aforementioned results highlight the role of EDEM3 in regulating LRP1 post-translational processing, and deletion of EDEM3 gene or the loss-of-function mutation facilitates the processing and transport of LRP1 to the cell surface.

### Hepatic EDEM3 KD in Mice Increased LRP1 Expression and Essentially Reduced Plasma TG Level

To obtain *in vivo* evidence for the regulation of EDEM3 in LRP1 expression, we knocked down EDEM3 expression in mouse livers using CRISPR/Cas9 genome editing system (Ran et al., 2015). We selected one sgRNA by *in vitro* screening a pool of sgRNAs that target EDEM3 exon 1 (see Methods). The sgRNA was cloned into a single vector adeno-associated virus (AAV)-Cas9 system containing *Staphylococcus aureus* Cas9 (SaCas9). The viral constructs

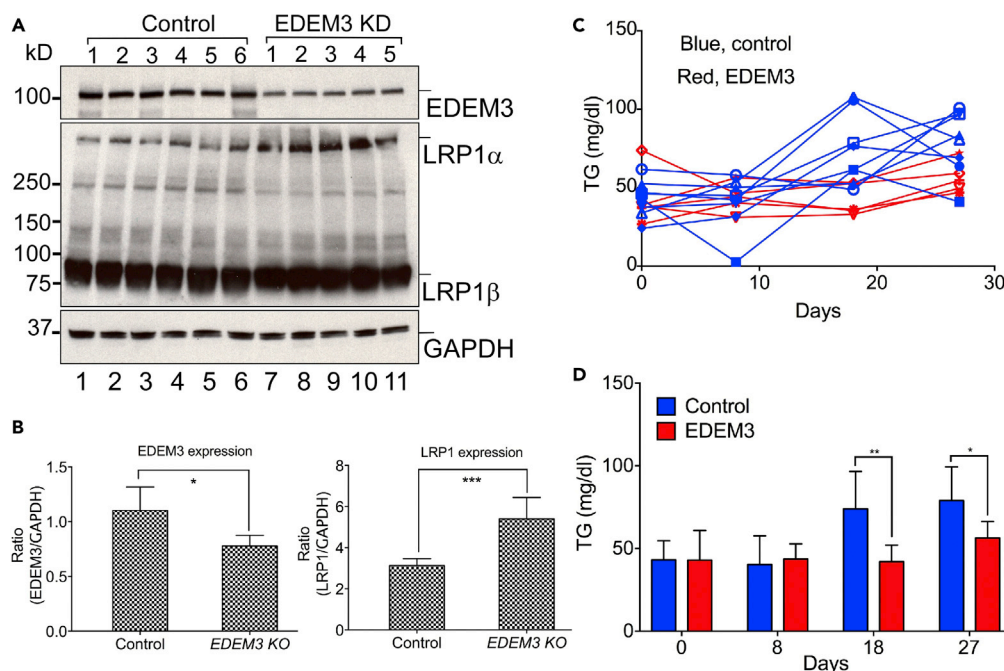


**Figure 8. Hepatic EDEM3 KD Increased LRP1 Expression and Reduced the Plasma TG Level in Mice**

(A) Liver extracts from the female mice injected with the control AAV or the AAV for EDEM3 CRISPR KD were analyzed with western blotting and probed with anti-EDEM3, anti-LRP1, and anti-GAPDH antibodies (from top to bottom).

(B) Quantification of EDEM3 and LRP1 expression normalized with GAPDH as in (A).

(C and D) Measurement of the plasma TG levels from the mice injected with the AAVs as in (A). (C) Individual mouse plasma TG levels; (D) average plasma TG of the control and EDEM3 KD groups. p values (t test) were calculated by comparing the KD mice with the corresponding control mice.

The error bars represent SEM in the figure. \*p < 0.05; \*\*p < 0.01; \*\*\*p < 0.001.

containing the EDEM3 sgRNA and a non-specific scramble sgRNA (control) were then used for AAV production. The AAV preparations were injected in WT female mice followed by high-fat diet.

Western analysis shows that the CRISPR-based KD reduced the hepatic EDEM3 expression (by ~50%) (Figure 8A, top and 8B, left). Also, the EDEM3 KD essentially reduced the plasma TG level on days 18 and 27 (by ~43% and ~29%, respectively) (Figures 8C and 8D). The higher plasma TG observed at days 18 and 27 in the control mice was likely induced by the high-fat diet. The TG reduction suggests that inhibition of EDEM3 might be able to decrease the diet-induced high TG level. Consistent with the above-mentioned results, EDEM3 KD significantly increased (by ~50%) the expression of hepatic LRP1 (Figure 8A, middle and 8B, right). Thus, we provide both *in vitro* and *in vivo* evidences that EDEM3 inhibition increases the expression of LRP1, which in turn increases the TGL uptake and reduces the plasma TG level.

### EDEM3 Deletion Increased the Expression of the Genes Required for RNA and Protein Processing and Transport

EDEM3 functions in protein quality control in the ER (Olivari and Molinari, 2007). Deletion of EDEM3 gene might affect the sensitivity of cells to ER stress. To test this, we treated EDEM3 KO and control HepG2 cells with tunicamycin, a reagent known to induce ER stress (Graham et al., 2016). The results (Figure S8) show that the treatment did not induce cell viability changes between the KO and control clones. We observed slightly more cell deaths only in one clone at the highest concentration of tunicamycin. Thus, the deficiency of EDEM3 might not add too much burden on protein processing in the ER.

It is likely that the KO cells might adapt some gene expression changes that enable them to tolerate the deficiency of EDEM3. To investigate this, we performed RNA sequencing (RNA-seq) analysis on the total RNA from the EDEM3 KO and WT HepG2 clones. Differential gene expression analysis shows that the

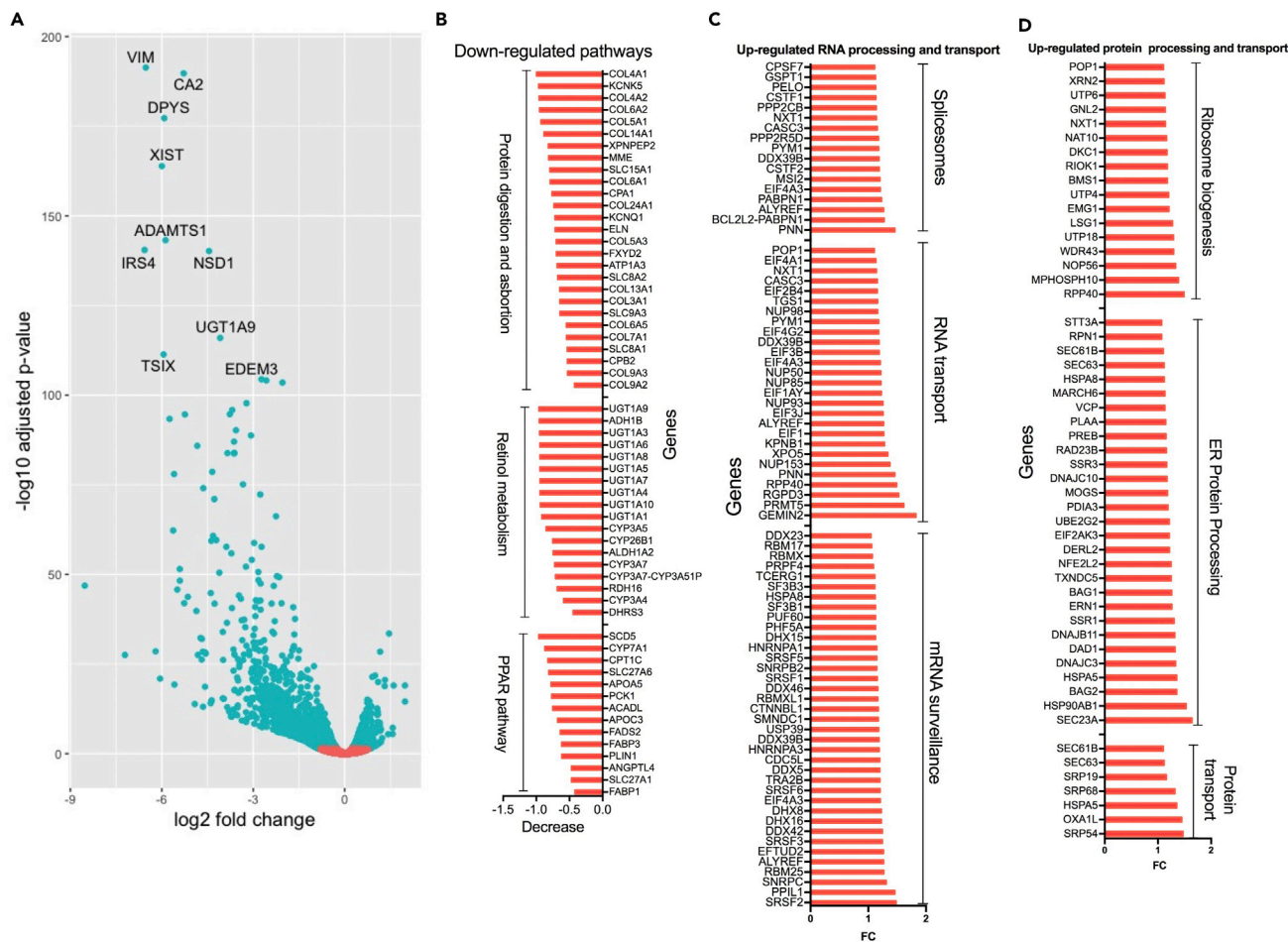


**Figure 9. Deletion of EDEM3 Gene in HepG2 cells Increased RNA and ER Protein Processing and Transport**  
 (A–C) Total RNA from three individual EDEM3 scramble control (WT) and KO HepG2 clones was analyzed with RNA-seq for differential gene expression (A). The down-regulated (B) and up-regulated (C and D) pathways related to EDEM3 gene deletion are shown.

EDEM3 gene deletion induced down-regulation of expression of a large number of genes (Figure 9A). The down-regulated gene expression resulted in reduced activities of many cellular metabolic pathways such as PPAR signaling, drug metabolism, and protein digestion and absorption (Figure 9B). Importantly, the pathway analyses show that the expression of the genes for RNA and protein processing and transport are up-regulated (Figures 9C and 9D). Thus, the up- and down-regulated pathways may directly alleviate the burden potentially resulting from the loss of EDEM3 protein in the ER and facilitate the LRP1 post-translational processing in the ER and transport on the cell surface.

**Plasma Metabolite Profile of rs78444298 (EDEM3 P746S) Corresponds to the Cellular Metabolite Pattern of EDEM3 Gene Deletion**

To investigate the lipid metabolite changes resulting from EDEM3 gene deletion, we used mass spectrometry to analyze the total lipid extracts from the EDEM3 KO and control HepG2 cells as previously reported (Mascanfroni et al., 2015; Xu et al., 2018). The results show that the gene deletion induced the accumulation of some diglycerides (DGs) and shorter-carbon-chain TGs (Figures 10A and 10B). For longer-carbon-chain TGs, some of them increased, whereas others decreased; however, if the cellular metabolite abundance is taken into consideration, there is still accumulation of the longer-carbon-chain TGs (Figure 10A). For instance, there are extremely low levels of C58:10 and C58:11 TGs. These TGs are much less abundant than the elevated TGs including C50:3, C52:1, C54:1, C54:2, C56:2, and C56:3. There is no significant change for the most abundant C52:2 TG.

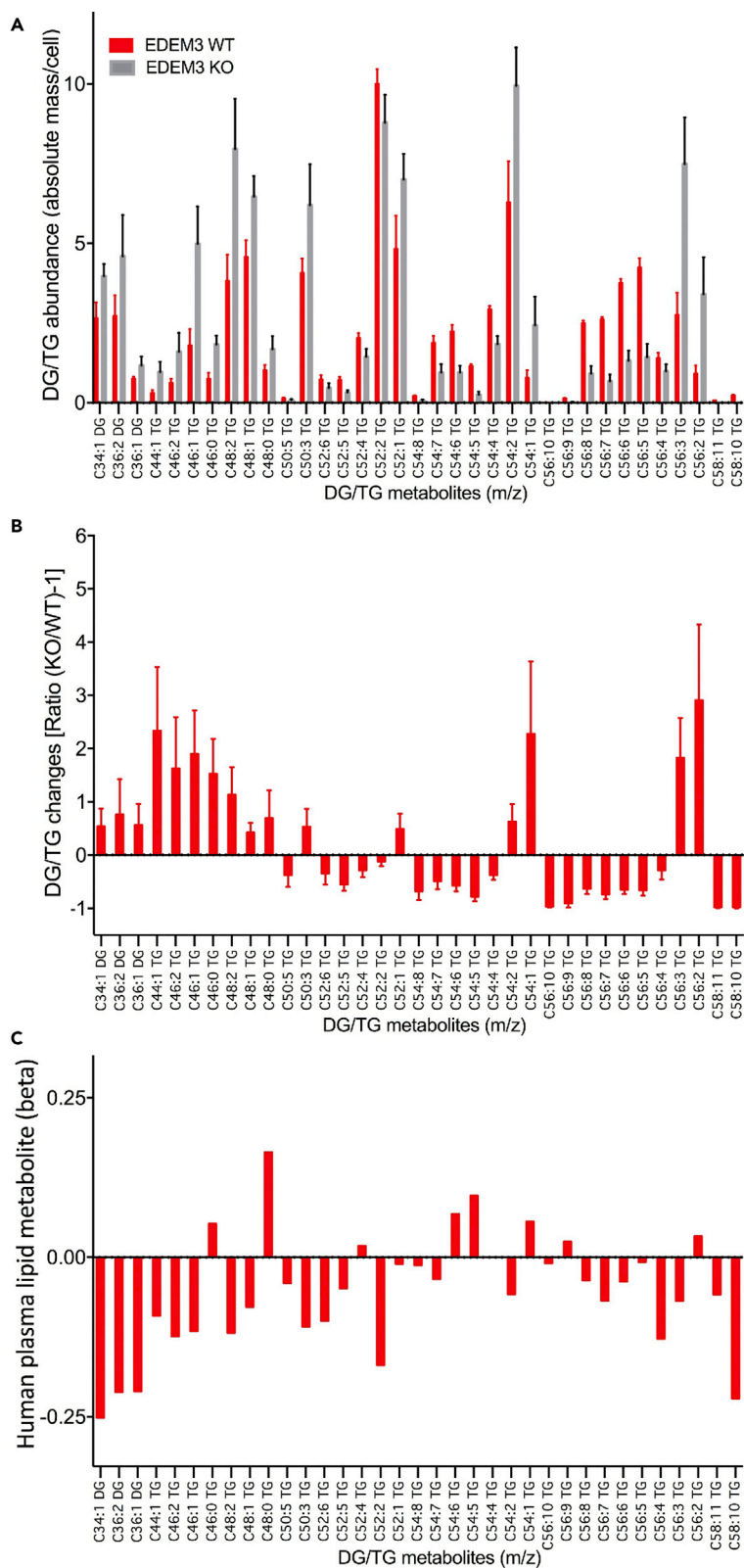


**Figure 10. Comparison of the Lipid Metabolite Profiles of rs78444298 (EDEM3 P746S) Framingham Heart Study (FHS) Individuals with Those from EDEM3 Gene Deletion in HepG2 Cells**

(A and B) Total cellular lipid extracts from three individual EDEM3 scramble control (WT) and KO HepG2 clones were analyzed with mass spectrometry. The metabolite profile was obtained by comparing the DG and TG abundances (A) and ratios (B) between the WT and KO cells.

(C) The association of plasma lipid metabolite profiles in 1,797 individuals from FHS with rs78444298 (P746S) from FHS 1000 Genomes genome-wide association study cohorts.

We next examined the plasma lipid metabolite changes by SNP rs78444298 genotype (G > A; 1.5% minor allele frequency) in 1,797 individuals from the Framingham Heart Study with 1000 Genomes imputed genotypes (Rhee et al., 2013). The results demonstrate a similar, but in opposite direction, pattern of DGs and shorter-carbon-chain TGs when compared with those from EDEM3 gene deletion (Figures 10B and 10C). More decreases were found for the longer-carbon-chain TGs. The longer and abundant TGs (C50:3, C52:1, C54:2, and C56:3), which were accumulated in the EDEM3 KO HepG2 clones, are negatively associated with the number of A alleles an individual carried, that is, as we modeled rs78444298 genotypes additively, individuals with the AG genotype have, on average, lower TG metabolites than the individuals with the GG genotype and individuals with the AA genotype have TG metabolites lower, on average, than individuals with the AG genotype. Thus, in general the plasma lipid metabolite profile with increasing number of A alleles is correlated with the corresponding pattern change of the EDEM3 gene deletion, in particular for those DGs and shorter-carbon-chain TGs. The decreased DGs and TGs might result from the increased uptake by the livers because of elevated LRP1 expression induced by the LoF EDEM3 mutation. However, more *in vivo* studies are needed to explore the lipid metabolic changes.

**DISCUSSION**

We demonstrate that an EDEM3 variant, P746S, is significantly associated with the lower blood TG level using human genetic data. We sought to use a cell-based functional approach by deleting the EDEM3 gene in human hepatoma cells to obtain mechanistic insight for this association. We found that the gene deletion strongly induced the uptake of VLDL as a result of up-regulated LRP1 expression. Hepatic EDEM3 KD in mice further confirmed the results *in vivo*. RNA-seq analyses reveal that the gene deletion up-regulated the pathways for RNA and ER protein processing, which likely facilitated the LRP1 processing in the ER and transport to the cell surface. Furthermore, our metabolomics data show that the cellular lipid metabolite profile is largely consistent with the counterpart association of the missense variant in the plasma of individuals from the population, suggesting that our functional analyses largely explain the phenotype from the genetic association. Collectively, we identified EDEM3 as a regulator in modulating plasma TGs via its activity in the ER, and thus it may represent a potential therapeutic target for TG lowering.

Blood TG level represents the TG content of TGLs in circulation, mainly including the remnants of chylomicron from dietary intake and VLDL secreted from the livers. Blood TG is associated with dietary fat intake, genetic determinants, and physical activity, as well as other factors. There are several drugs available for the treatment of hypertriglyceridemia such as niacin, fibrates, and omega-3-fatty acids (Cooper et al., 2015; Group et al., 2018; Pawlak et al., 2015), but none of them is specific. Finding targets for lowering TG and further using them for drug development have lagged behind the drug development for LDL-C lowering. Recent human genetic studies have identified ApoC3 and ANGPTL3 as two important TG targets (Jorgensen et al., 2014; Musunuru et al., 2010; Crosby et al., 2014). Inhibition of ApoC3 and ANGPTL3 showed strong effects in lowering the blood TG (Gaudet et al., 2014, 2017; Xu et al., 2018). However, the two targets share a similar mechanism in modulating the blood TG, i.e., the inhibition of LPL. As mentioned earlier, the three top LDL-C-lowering drugs, statin, ezetimibe, and the PCSK9 inhibitor, cover the hepatic cholesterol synthesis, intestinal cholesterol absorption, and LDL uptake, respectively (Ajufo and Rader, 2016). Combination use of these drugs will provide great strength for treatment of complex hyperlipidemia, which cannot be controlled by a single therapeutic agent. Thus, the finding of EDEM3 and its role in modulating blood TG via regulating LRP1 expression would complement the current TG-lowering therapeutic efforts.

EDEM3 modulates the plasma TG by regulating LRP1 expression, which is consistent with the role of LRP1 in regulating TG metabolism (Lillis et al., 2008). In contrast to the LDLR, which binds to ApoB-100 as well as ApoE, LRP1 mediates the hepatic uptake of the TGLs mainly through its binding with ApoE, which is present in both chylomicrons and VLDL (Beisiegel, 1998; Mahley and Huang, 2007). It was observed that

genetic defects of LDLR both in humans and mice cause hypercholesterolemia by reducing the uptake of cholesterol-rich LDL, but the clearance of TGLs is not affected (Kita et al., 1982; Rubinsztein et al., 1990). High plasma TG was only observed when the LRP1 expression is inactivated under LDLR deficiency (Rohlmann et al., 1998; Willnow et al., 1995). Although the mechanisms for LRP1 and LDLR in regulating TG metabolism remain to be determined (Rohlmann et al., 1998), the existing data suggest that LRP1 plays a major role in the clearance of TGLs.

EDEM3 likely regulates LRP1 expression in a post-transcriptional manner because our RNA-seq analysis did not show significant differences in LRP1 mRNA transcript levels between the EDEM3 WT and KO cells (Figure 9). It was previously shown that all the LDLR family members including LRP1 possess N-linked glycosylation (May et al., 2003). LRP1 is differentially glycosylated apparently only with N-linked glycans in a tissue-specific manner. Although the extent and distribution of the differential glycosylations are largely unknown, it may explain the difference of mobility changes of the LRP1 proteins from HepG2 and Huh7 EDEM3 KO cells (Figures 6A and 6B). The mannose-containing N-linked glycans are co-translationally added to the nascent receptor polypeptides, which serves as signals recognized by the ER-resident chaperones and folding factors to ensure proper maturation. The unrecoverable misfolded polypeptides undergo mannose trimming by the GH47 family mannosidases including EDEM1, 2, and 3 and are then eventually translocated from the lumen of the ER into the cytoplasm for degradation. EDEM proteins play important roles in maintaining protein folding efficiency by facilitating the extraction of misfolded glycoproteins and accelerating the onset of their degradation.

It is intriguing that the EDEM3 deficiency increases the cell surface LRP1 expression. It could be speculated that EDEM3 deficiency may accelerate the processing and transport of LRP1 from the ER. The acceleration may rely on the N-linked glycan of LRP1 and the  $\alpha$ 1,2 mannosidase activity of EDEM3, which trim the  $\alpha$ (1,2) mannoses of the glycans (Hirao et al., 2006), a crucial step in determining the fate of misfolded proteins between productive folding and degradation (Olivari and Molinari, 2007). Under EDEM3 deficiency, the LRP1 may carry more mannose moieties at the N-linked glycans, which may allow the LRP1 to evade the ER quality surveillance and transport on the cell surface more efficiently. The direct evidence supporting this hypothesis is that the LRP1 under EDEM3 deficiency showed slower mobility likely due to more mannoses that evaded from the trimming (Figures 6A and 7A), and there were more mannoses on the cell surface of HepG2 EDEM3 KO cells (Figure 6C).

All three EDEM members were reported to have the mannosidase activity lately (Hosokawa et al., 2010; Shenkman et al., 2018). It is not clear, however, how the apparently redundant enzymes function differentially in the ER mannose trimming. Our genetic and mechanistic studies here provide some clues that EDEM3 plays more important roles than previously thought. Nevertheless, EDEM3 has some unique structural features that are missing in the other members. It has a PA domain and an ER retrieval signal (Figure 2C) (Olivari and Molinari, 2007). The ER signal may constantly keep EDEM3 in the ER lumen. Interestingly, the P746S mutation is exactly located at the PA domain of EDEM3 coding region (Figure 2C). Notably, many proteases have the PA domains in their noncatalytic regions, which bear high homology in the domain sequences (Luo and Hofmann, 2001). Although little is known about this domain of EDEM3, studies from other PA-containing proteases suggest that these domains play important roles in determining the protein functions such as in substrate targeting and autoinhibitor. Thus, EDEM3 could be the only mannosidase that targets specific protein substrates in the compartment of ER, although more work need to be done to clarify the mechanism.

Our studies indicate that the deletion of EDEM3 gene did not alter the cellular response to the induced ER stress *in vitro* (Figure S8), suggesting that under normal growth condition, there might not be many misfolded proteins accumulated in the ER of the KO cells when compared with the WT cells. This may reflect that the change of gene expression resulted from the EDEM3 gene deletion. We observed that the expression of the genes responsible for cellular metabolic pathways was down-regulated, whereas the expression of the genes involved in the RNA and ER protein processing and transport was up-regulated. These gene expression changes may be able to compensate any defects in the ER caused by the loss of EDEM3 protein. However, the expression of the downstream genes regulated by unfolded protein response (UPR) pathways is virtually no different between the KO and WT cells. For instance, no significant changes were found for the expression of the transcription factor ATF6 and its target genes such BiP, protein disulfide isomerase, and glucose-regulated protein 94, which are the key ER-resident proteins for protein folding (Bernasconi and Molinari, 2011; Walter and Ron, 2011). Additionally, in a typical UPR, the mRNA translation

is inhibited to reduce the protein loading in the ER under ER stress. In this case the mRNA and protein production was up-regulated in the EDEM3 KO cells. Thus, the gene expression change may not be related to UPR. The increased RNA and protein production may be the response of the KO cells to compensate the reduced capacity in the protein processing due to the EDEM3 deficiency.

Genetic factors contribute to over 20% of the inter-individual variation of human plasma metabolites (Gieger et al., 2008; Rhee et al., 2013). Given the key roles of metabolites as markers and effectors in cardiovascular diseases, it has become increasingly important to interrogate machineries and mechanisms behind the metabolite variations from population-based cohorts via genetic and biological studies. In this study, we leveraged human metabolomics data in over 1,500 individuals. We compared the association of EDEM3 P746S plasma lipid metabolite profile with the corresponding cellular pattern of the EDEM3 KO cells. They are largely correlated, suggesting that the up-regulated LRP1-mediated TGL uptake may have a major impact on the human TG phenotype. Although further studies are needed to obtain a broad spectrum of human plasma metabolite data and expand the studies on the functions of EDEM3 in regulating the cellular lipid metabolism, our study provides an example of how human genetic, functional and mechanistic, and human metabolomics studies can be emphasized for a broad biological insight with respect of disease pathogenesis of a gene.

In summary, in this study, by using a population-based genetic approach, we first demonstrated that a missense mutation in the coding region of EDEM3 is significantly associated with lower plasma TG in a large association study. We then performed both *in vitro* and *in vivo* functional analyses by either deleting EDEM3 gene in human hepatoma cell lines or hepatic EDEM3 KD in mice. We observed that the inhibition of EDEM3 expression increased LRP1 expression, which in turn induced TGL uptake and further reduced the plasma TG level. Finally, our metabolomics analysis indicates that EDEM3 deficiency increased cellular TG accumulation, which is inversely associated with the lipid metabolite profile of the plasma from the individuals carrying the EDEM3 alternate allele, suggesting that the LRP1-mediated TGL uptake plays a major role in the TG phenotype. Importantly, EDEM3 inhibition increased the expression of genes involved in the RNA and ER protein processing and transport, without altering the sensitivity of cells to ER stress, indicating that inhibition of EDEM3 expression could be potentially used as therapeutic approach to treat hypertriglyceridemia.

### Limitation of the Study

Although multiple lines of evidence including from human genetics, *in vitro* cell, *in vivo* mouse models, and human metabolomics were provided to validate the roles of EDEM3 in regulating LRP1 expression, further studies are needed to obtain more mechanistic insight about this regulation. It will be especially important to investigate the correlation of EDEM3 inhibition with increasing LRP1 expression and reducing blood TG level for targeting EDEM3 with the goal of TG-lowering treatments. Our *in vivo* data from the mouse work only displayed modest impact on the TG level largely due of the limited reduction in EDEM3 expression from CRISPR gene silencing. We would expect stronger effect on TG lowering if substantial reduction in EDEM3 expression is obtained. Our human metabolomics data were obtained only from the limited number of individuals carrying the EDEM3 mutation with blood lipid metabolite measurements. Expanding the human genetic study together with lipid metabolomics on EDEM3 would shed broader insight about the regulation of EDEM3 in lipid metabolism at the population level, which would enable us to understand how the regulation correlates with the mechanistic data from *in vitro* and *in vivo* analyses.

### METHODS

All methods can be found in the accompanying [Transparent Methods supplemental file](#).

### DATA AND CODE AVAILABILITY

The RNA-seq data presented in this article are deposited in Gene Expression Omnibus (GEO). The accession number for the data reported in this paper is GSE146070. The link to the data is at <https://www.ncbi.nlm.nih.gov/geo/query/acc.cgi?acc=GSE146070>.

### SUPPLEMENTAL INFORMATION

Supplemental Information can be found online at <https://doi.org/10.1016/j.isci.2020.100973>.

## ACKNOWLEDGMENTS

This work was supported by funding from National Heart, Lung, and Blood Institute grant 5R33HL120781-05 to S.K. G.M.P. is supported by KO1HL125751, RO3HL141439, and RO1HL142711. X.-Y.X. was in part supported by American Heart Association SDG grant (11SDG7670007). We thank Partners Healthcare Personalized Medicine for the RNA-seq acquisition and analysis, in particular Dr. Sami Samir Amr and Mark J. Bowser for their support in the data analysis and submission, and Andrew Johnston for his contribution to the early stage of this project.

## AUTHOR CONTRIBUTIONS

Conceptualization, X.-Y.X. and S.K.; Methodology, X.-Y.X., G.M.P., K.M., C.B.C., D.R., and S.K.; Formal analysis, X.-Y.X., G.M.P., H.L., T.H.N., A.D., and K.B.; Investigation, X.-Y.X., G.M.P., T.H.N., T.M., A.D., and K.B.; Resources, Q.Y., R.S.V., and R.E.G.; Writing – Original draft, X.Y.X.; Writing – Editing, X.-Y.X., G.M.P., T.M., A.D., H.L., R.S.V., and S.K.; Writing – Supervision, X.-Y.X. and S.K..

## DECLARATION OF INTERESTS

The authors declare no competing interests.

Received: October 8, 2019

Revised: December 6, 2019

Accepted: March 5, 2020

Published: April 24, 2020

## REFERENCES

- Ajufo, E., and Rader, D.J. (2016). Recent advances in the pharmacological management of hypercholesterolaemia. *Lancet Diabetes Endocrinol.* 4, 436–446.
- Bauer, R.C., Khetarpal, S.A., Hand, N.J., and Rader, D.J. (2016). Therapeutic targets of triglyceride metabolism as informed by human genetics. *Trends Mol. Med.* 22, 328–340.
- Beisiegel, U. (1998). Lipoprotein metabolism. *Eur. Heart J.* 19, A20–A23.
- Bernasconi, R., and Molinari, M. (2011). ERAD and ERAD tuning: disposal of cargo and of ERAD regulators from the mammalian ER. *Curr. Opin. Cell Biol* 23, 176–183.
- Cooper, D.L., Murrell, D.E., Roane, D.S., and Harirforoosh, S. (2015). Effects of formulation design on niacin therapeutics: mechanism of action, metabolism, and drug delivery. *Int. J. Pharm.* 490, 55–64.
- Do, R., Willer, C.J., Schmidt, E.M., Sengupta, S., Gao, C., Peloso, G.M., Gustafsson, S., Kanoni, S., Ganna, A., Chen, J., et al. (2013). Common variants associated with plasma triglycerides and risk for coronary artery disease. *Nat. Genet.* 45, 1345–1352.
- Eriksson, K.K., Vago, R., Calanca, V., Galli, C., Paganetti, P., and Molinari, M. (2004). EDEM contributes to maintenance of protein folding efficiency and secretory capacity. *J. Biol. Chem.* 279, 44600–44605.
- Frykman, P.K., Brown, M.S., Yamamoto, T., Goldstein, J.L., and Herz, J. (1995). Normal plasma lipoproteins and fertility in gene-targeted mice homozygous for a disruption in the gene encoding very low density lipoprotein receptor. *Proc. Natl. Acad. Sci. U S A* 92, 8453–8457.
- Gaudet, D., Brisson, D., Tremblay, K., Alexander, V.J., Singleton, W., Hughes, S.G., Geary, R.S., Baker, B.F., Graham, M.J., Crooke, R.M., et al. (2014). Targeting APOC3 in the familial chylomicronemia syndrome. *N. Engl. J. Med.* 371, 2200–2206.
- Gaudet, D., Gipe, D.A., Pordy, R., Ahmad, Z., Cuchel, M., Shah, P.K., Chyu, K.Y., Sasiela, W.J., Chan, K.C., Brisson, D., et al. (2017). ANGPTL3 inhibition in homozygous familial hypercholesterolemia. *N. Engl. J. Med.* 377, 296–297.
- Gieger, C., Geistlinger, L., Altmaier, E., Hrabce de Angelis, M., Kronenberg, F., Meitinger, T., Mewes, H.W., Wichmann, H.E., Weinberger, K.M., Adamski, J., et al. (2008). Genetics meets metabolomics: a genome-wide association study of metabolite profiles in human serum. *Plos Genet.* 4, e1000282.
- Graham, D.B., Lefkovich, A., Deelen, P., de Klein, N., Varma, M., Boroughs, A., Desch, A.N., Ng, A.C.Y., Guzman, G., Schenone, M., et al. (2016). TMEM258 is a component of the oligosaccharyltransferase complex controlling ER stress and intestinal inflammation. *Cell Rep* 17, 2955–2965.
- Group, A.S.C., Bowman, L., Mafham, M., Wallendszus, K., Stevens, W., Buck, G., Barton, J., Murphy, K., Aung, T., Haynes, R., et al. (2018). Effects of n-3 fatty acid supplements in diabetes mellitus. *N. Engl. J. Med.* 379, 1540–1550.
- Hebert, D.N., Garman, S.C., and Molinari, M. (2005). The glycan code of the endoplasmic reticulum: asparagine-linked carbohydrates as protein maturation and quality-control tags. *Trends Cell Biol* 15, 364–370.
- Hirao, K., Natsuka, Y., Tamura, T., Wada, I., Morito, D., Natsuka, S., Romero, P., Sleno, B., Tremblay, L.O., Herscovics, A., et al. (2006). EDEM3, a soluble EDEM homolog, enhances glycoprotein endoplasmic reticulum-associated degradation and mannose trimming. *J. Biol. Chem.* 281, 9650–9658.
- Hosokawa, N., Tremblay, L.O., Sleno, B., Kamiya, Y., Wada, I., Nagata, K., Kato, K., and Herscovics, A. (2010). EDEM1 accelerates the trimming of alpha1,2-linked mannose on the C branch of N-glycans. *Glycobiology* 20, 567–575.
- Johansen, C.T., Kathiresan, S., and Hegele, R.A. (2011). Genetic determinants of plasma triglycerides. *J. Lipid Res.* 52, 189–206.
- Jorgensen, A.B., Frikke-Schmidt, R., Nordestgaard, B.G., and Tybjaerg-Hansen, A. (2014). Loss-of-function mutations in APOC3 and risk of ischemic vascular disease. *N. Engl. J. Med.* 371, 32–41.
- Kita, T., Goldstein, J.L., Brown, M.S., Watanabe, Y., Hornick, C.A., and Havel, R.J. (1982). Hepatic uptake of chylomicron remnants in WHHL rabbits: a mechanism genetically distinct from the low density lipoprotein receptor. *Proc. Natl. Acad. Sci. U S A* 79, 3623–3627.
- Larsson, M., Vorrso, E., Talmud, P., Lookene, A., and Olivecrona, G. (2013). Apolipoproteins C-I and C-III inhibit lipoprotein lipase activity by displacement of the enzyme from lipid droplets. *J. Biol. Chem.* 288, 33997–34008.
- Lee, E.C., Desai, U., Gololobov, G., Hong, S., Feng, X., Yu, X.C., Gay, J., Wilganowski, N., Gao, C., Du, L.L., et al. (2009). Identification of a new functional domain in angiotensin-like 3 (ANGPTL3) and angiotensin-like 4 (ANGPTL4) involved in binding and inhibition of lipoprotein lipase (LPL). *J. Biol. Chem.* 284, 13735–13745.

- Lillis, A.P., Van Duyn, L.B., Murphy-Ullrich, J.E., and Strickland, D.K. (2008). LDL receptor-related protein 1: unique tissue-specific functions revealed by selective gene knockout studies. *Physiol. Rev.* 88, 887–918.
- Liu, D.J., Peloso, G.M., Yu, H., Butterworth, A.S., Wang, X., Mahajan, A., Saleheen, D., Emdin, C., Alam, D., Alves, A.C., et al. (2017). Exome-wide association study of plasma lipids in >300,000 individuals. *Nat. Genet.* 49, 1758–1766.
- Luo, X., and Hofmann, K. (2001). The protease-associated domain: a homology domain associated with multiple classes of proteases. *Trends Biochem. Sci.* 26, 147–148.
- Mahley, R.W., and Huang, Y. (2007). Atherogenic remnant lipoproteins: role for proteoglycans in trapping, transferring, and internalizing. *J. Clin. Invest.* 117, 94–98.
- Malik, S., Wong, N.D., Franklin, S.S., Kamath, T.V., L'Italien, G.J., Pio, J.R., and Williams, G.R. (2004). Impact of the metabolic syndrome on mortality from coronary heart disease, cardiovascular disease, and all causes in United States adults. *Circulation* 110, 1245–1250.
- Mascanfroni, I.D., Takenaka, M.C., Yeste, A., Patel, B., Wu, Y., Kenison, J.E., Siddiqui, S., Basso, A.S., Otterbein, L.E., Pardoll, D.M., et al. (2015). Metabolic control of type 1 regulatory T cell differentiation by AHR and HIF1- $\alpha$ . *Nat. Med.* 21, 638–646.
- May, P., Bock, H.H., Nimpf, J., and Herz, J. (2003). Differential glycosylation regulates processing of lipoprotein receptors by gamma-secretase. *J. Biol. Chem.* 278, 37386–37392.
- Musunuru, K., Pirruccello, J.P., Do, R., Peloso, G.M., Guiducci, C., Sougnez, C., Garimella, K.V., Fisher, S., Abreu, J., Barry, A.J., et al. (2010). Exome sequencing, ANGPTL3 mutations, and familial combined hypolipidemia. *New Engl. J. Med.* 363, 2220–2227.
- Nimpf, J., and Schneider, W.J. (2000). From cholesterol transport to signal transduction: low density lipoprotein receptor, very low density lipoprotein receptor, and apolipoprotein E receptor-2. *Biochim. Biophys. Acta* 1529, 287–298.
- Olivari, S., and Molinari, M. (2007). Glycoprotein folding and the role of EDEM1, EDEM2 and EDEM3 in degradation of folding-defective glycoproteins. *FEBS Lett.* 581, 3658–3664.
- Ono, M., Shimizugawa, T., Shimamura, M., Yoshida, K., Noji-Sakikawa, C., Ando, Y., Koishi, R., and Furukawa, H. (2003). Protein region important for regulation of lipid metabolism in angiotensin-like 3 (ANGPTL3): ANGPTL3 is cleaved and activated in vivo. *J. Biol. Chem.* 278, 41804–41809.
- Pawlak, M., Lefebvre, P., and Staels, B. (2015). Molecular mechanism of PPAR $\alpha$  action and its impact on lipid metabolism, inflammation and fibrosis in non-alcoholic fatty liver disease. *J. Hepatol.* 62, 720–733.
- Ramms, B., and Gordts, P. (2018). Apolipoprotein C-III in triglyceride-rich lipoprotein metabolism. *Curr. Opin. Lipidol.* 29, 171–179.
- Ran, F.A., Cong, L., Yan, W.X., Scott, D.A., Gootenberg, J.S., Kriz, A.J., Zetsche, B., Shalem, O., Wu, X., Makarova, K.S., et al. (2015). In vivo genome editing using *Staphylococcus aureus* Cas9. *Nature* 520, 186–191.
- Rhee, E.P., Ho, J.E., Chen, M.H., Shen, D., Cheng, S., Larson, M.G., Ghorbani, A., Shi, X., Helenius, I.T., O'Donnell, C.J., et al. (2013). A genome-wide association study of the human metabolome in a community-based cohort. *Cell Metab* 18, 130–143.
- Rohlmann, A., Gotthardt, M., Hammer, R.E., and Herz, J. (1998). Inducible inactivation of hepatic LRP gene by cre-mediated recombination confirms role of LRP in clearance of chylomicron remnants. *J. Clin. Invest.* 101, 689–695.
- Rubinsztein, D.C., Cohen, J.C., Berger, G.M., van der Westhuyzen, D.R., Coetzee, G.A., and Gevers, W. (1990). Chylomicron remnant clearance from the plasma is normal in familial hypercholesterolemic homozygotes with defined receptor defects. *J. Clin. Invest.* 86, 1306–1312.
- Sanjana, N.E., Shalem, O., and Zhang, F. (2014). Improved vectors and genome-wide libraries for CRISPR screening. *Nat. Methods* 11, 783–784.
- Shalem, O., Sanjana, N.E., Hartenian, E., Shi, X., Scott, D.A., Mikkelsen, T.S., Heckl, D., Ebert, B.L., Root, D.E., Doench, J.G., et al. (2014). Genome-scale CRISPR-Cas9 knockout screening in human cells. *Science* 343, 84–87.
- Shenkman, M., Ron, E., Yehuda, R., Benyair, R., Khalaila, I., and Lederkremer, G.Z. (2018). Mannosidase activity of EDEM1 and EDEM2 depends on an unfolded state of their glycoprotein substrates. *Commun. Biol.* 1, 172.
- Stephan, Z.F., and Yurachek, E.C. (1993). Rapid fluorometric assay of LDL receptor activity by Dil-labeled LDL. *J. Lipid Res* 34, 325–330.
- TG and HDL Working Group of the Exome Sequencing Project, National Heart, Lung, and Blood Institute, Crosby, J., Peloso, G.M., Auer, P.L., Crosslin, D.R., Stitzel, N.O., Lange, L.A., Lu, Y., et al. (2014). Loss-of-function mutations in APOC3, triglycerides, and coronary disease. *N. Engl. J. Med.* 371, 22–31.
- Trombetta, E.S., and Parodi, A.J. (2003). Quality control and protein folding in the secretory pathway. *Annu. Rev. Cell Dev Biol* 19, 649–676.
- Walter, P., and Ron, D. (2011). The unfolded protein response: from stress pathway to homeostatic regulation. *Science* 334, 1081–1086.
- Willer, C.J., Schmidt, E.M., Sengupta, S., Peloso, G.M., Gustafsson, S., Kanoni, S., Ganna, A., Chen, J., Buchkovich, M.L., Mora, S., et al. (2013). Discovery and refinement of loci associated with lipid levels. *Nat. Genet.* 45, 1274–1283.
- Willnow, T.E., Armstrong, S.A., Hammer, R.E., and Herz, J. (1995). Functional expression of low density lipoprotein receptor-related protein is controlled by receptor-associated protein in vivo. *Proc. Natl. Acad. Sci. U S A.* 92, 4537–4541.
- Willnow, T.E., Sheng, Z., Ishibashi, S., and Herz, J. (1994). Inhibition of hepatic chylomicron remnant uptake by gene transfer of a receptor antagonist. *Science* 264, 1471–1474.
- Xu, Y.X., Liu, L., Caffaro, C.E., and Hirschberg, C.B. (2010). Inhibition of Golgi apparatus glycosylation causes endoplasmic reticulum stress and decreased protein synthesis. *J. Biol. Chem.* 285, 24600–24608.
- Xu, Y.X., Redon, V., Yu, H., Querbes, W., Pirruccello, J., Liebow, A., Deik, A., Trindade, K., Wang, X., Musunuru, K., et al. (2018). Role of angiotensin-like 3, ANGPTL3, in regulating plasma level of low-density lipoproteins. *Atherosclerosis* 268, 196–206.

iScience, Volume 23

## **Supplemental Information**

### **EDEM3 Modulates Plasma**

### **Triglyceride Level through Its Regulation**

### **of LRP1 Expression**

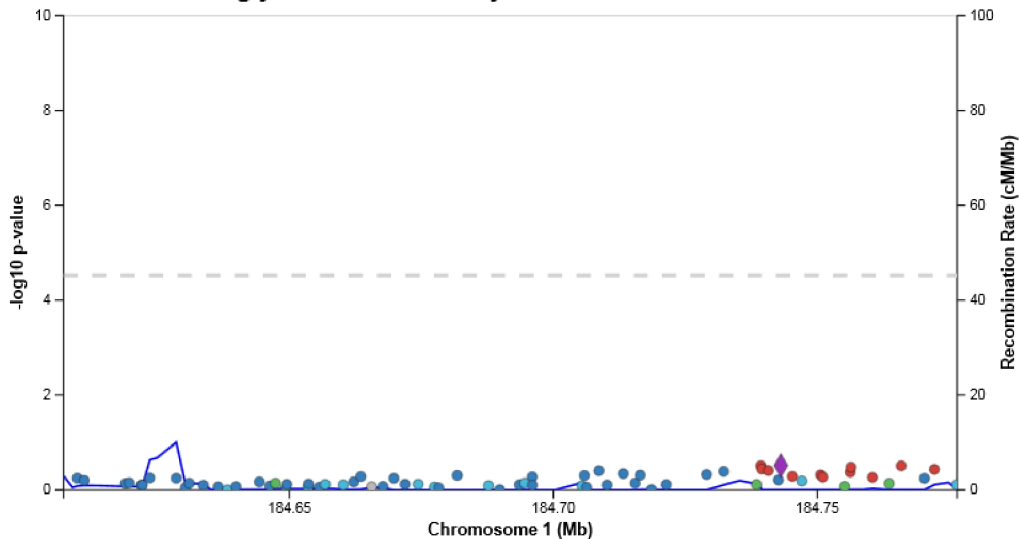
**Yu-Xin Xu, Gina M. Peloso, Taylor H. Nagai, Taiji Mizoguchi, Amy Deik, Kevin Bullock, Honghuang Lin, Kiran Musunuru, Qiong Yang, Ramachandran S. Vasan, Robert E. Gerszten, Clary B. Clish, Daniel Rader, and Sekar Kathiresan**

## **Supplemental information**

Supplemental information contains supplemental figures S1-S8, supplemental figure legends, supplemental table S1, and transparent methods including key resource table.

# Figure S1

## Willer CJ 2013 - Triglycerides meta-analysis



*SNORD112* →



← *FAM129A*



← *EDEM3*



Figure S2

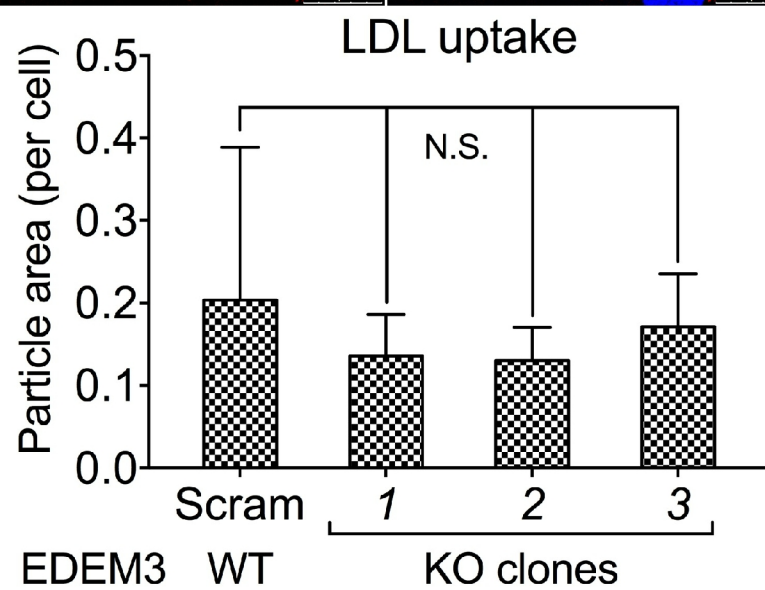
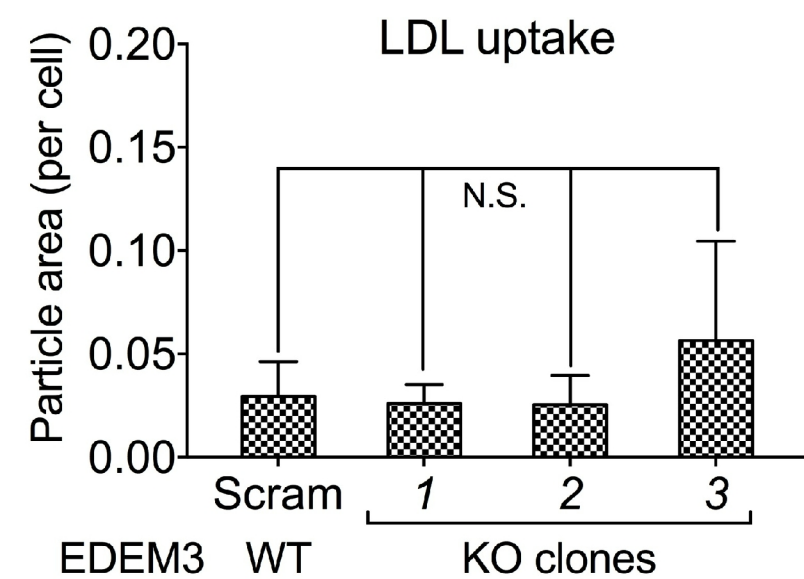
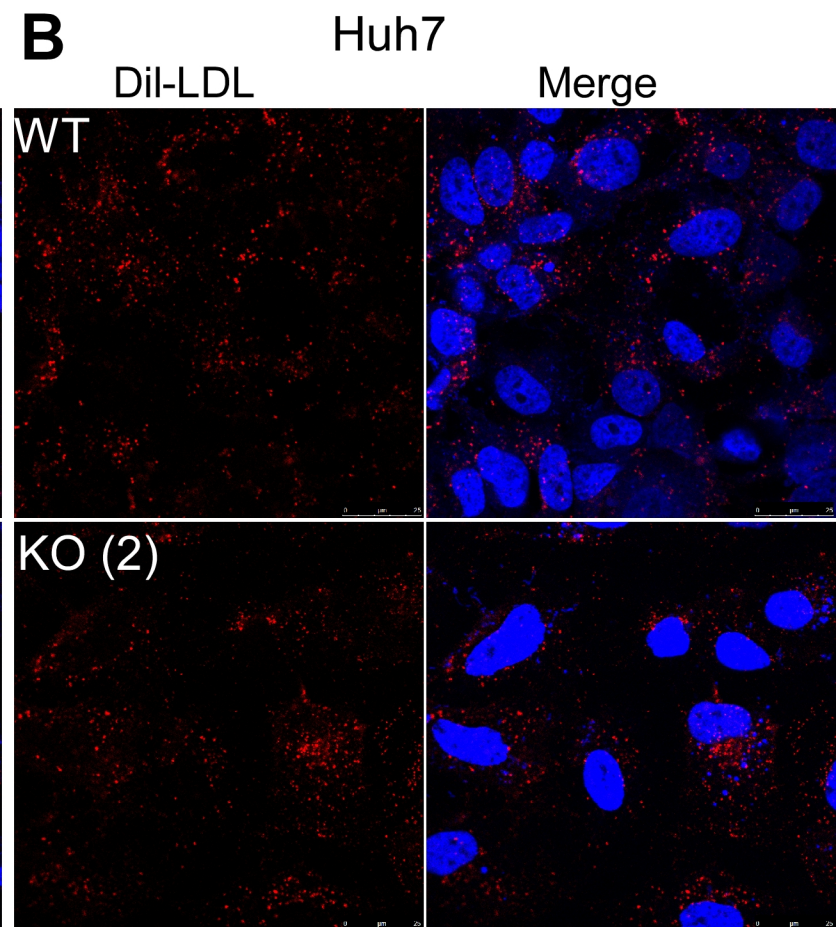
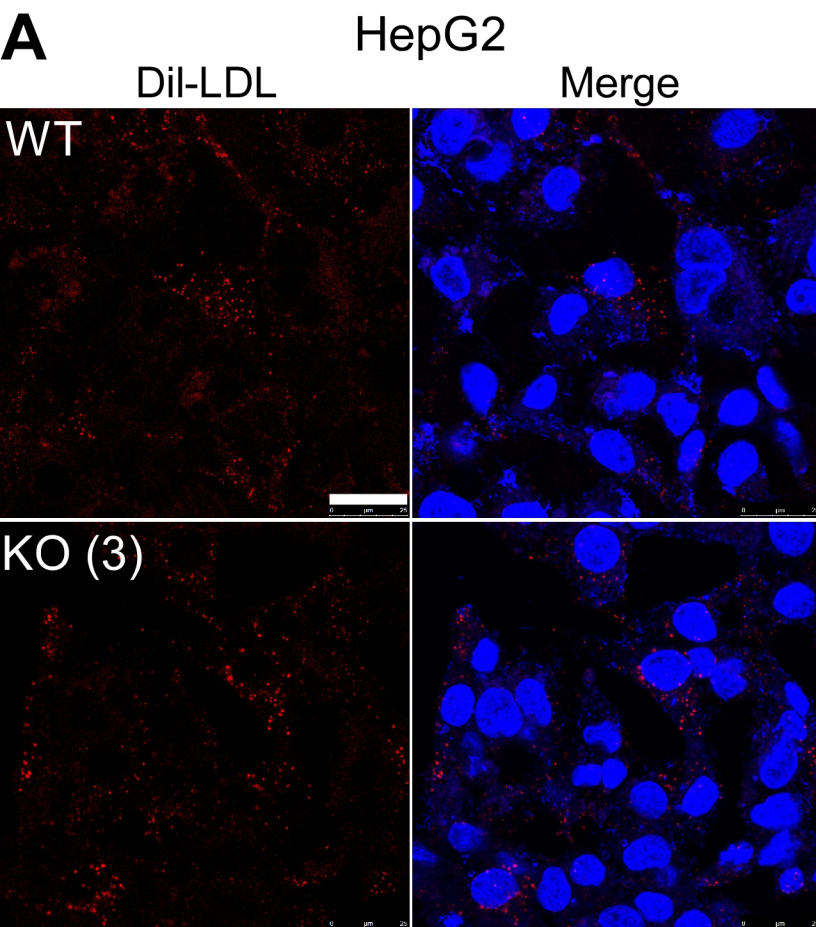


Figure S3

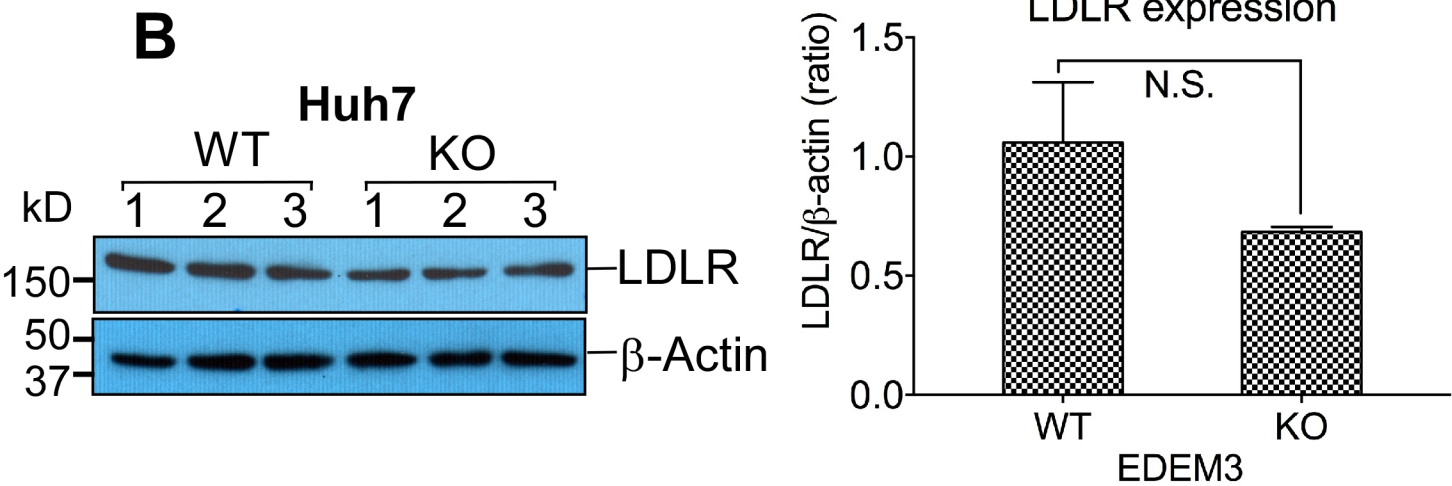
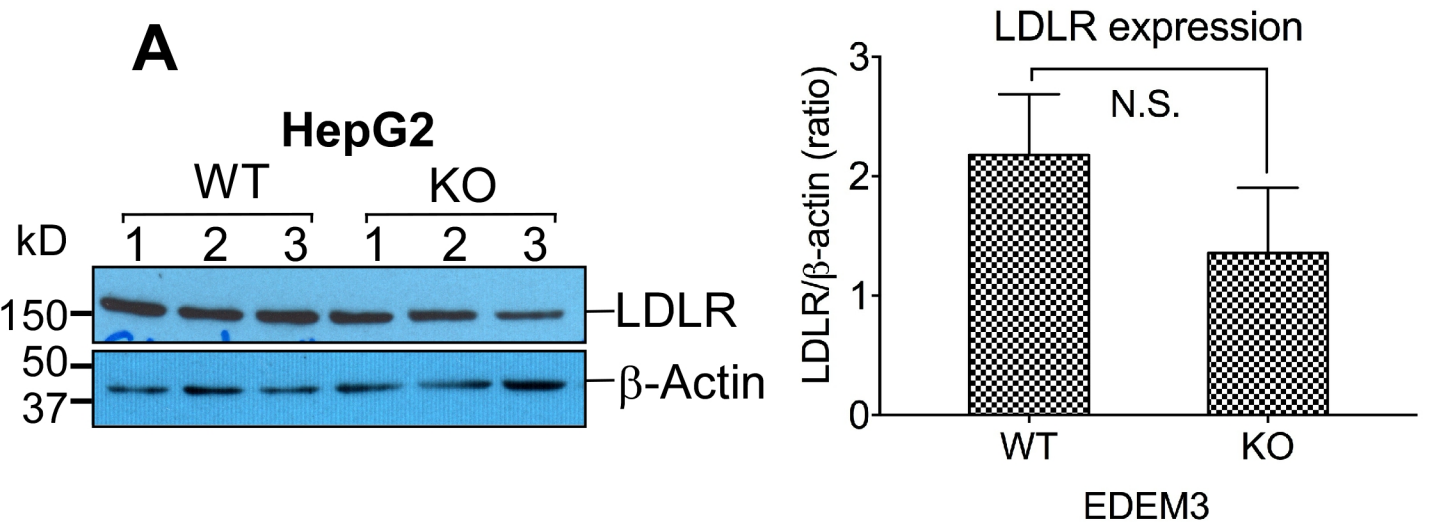


Figure S4

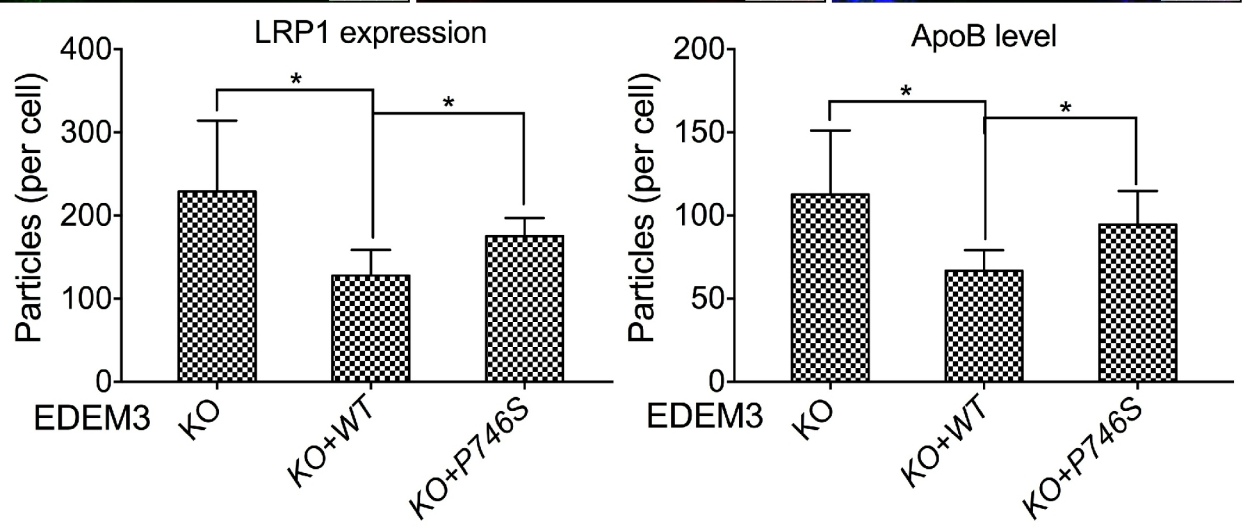
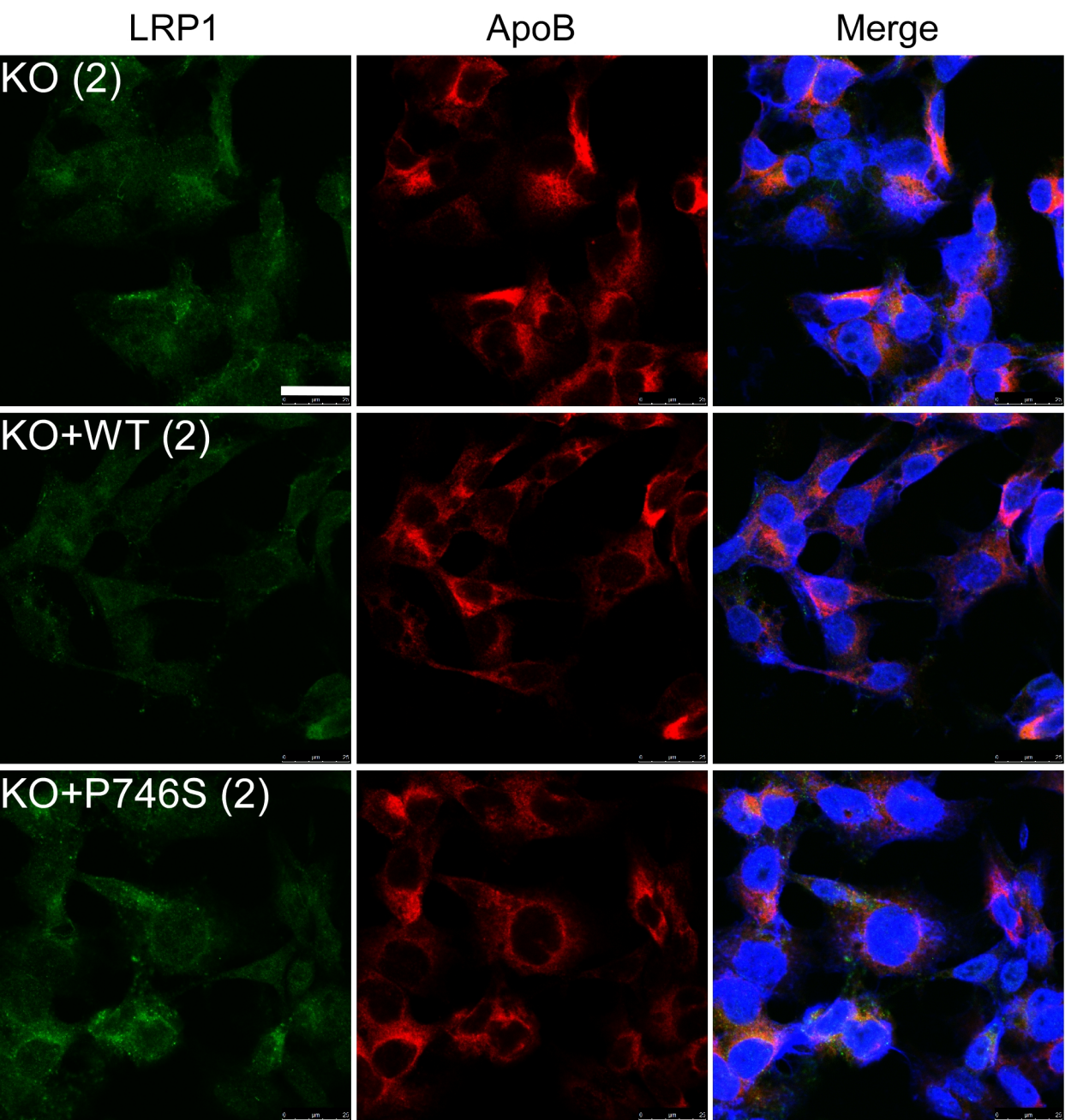


Figure S5

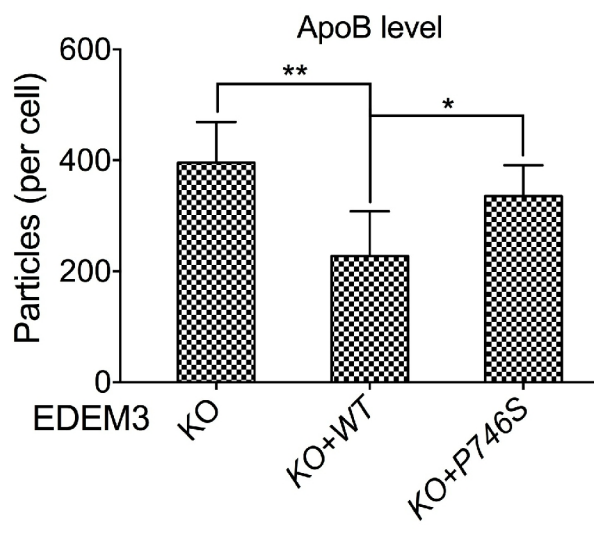
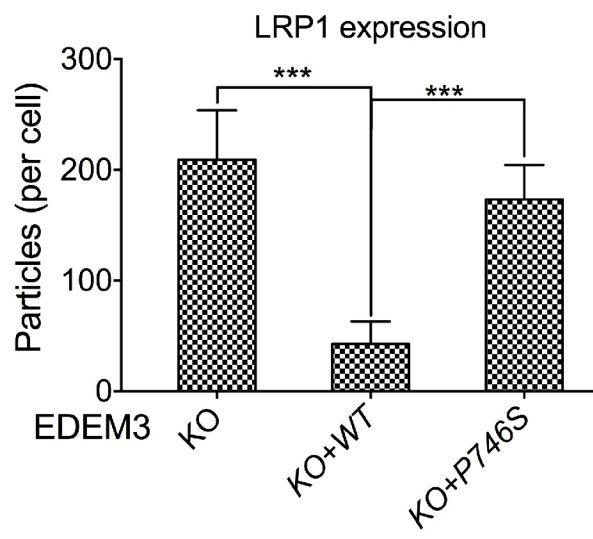
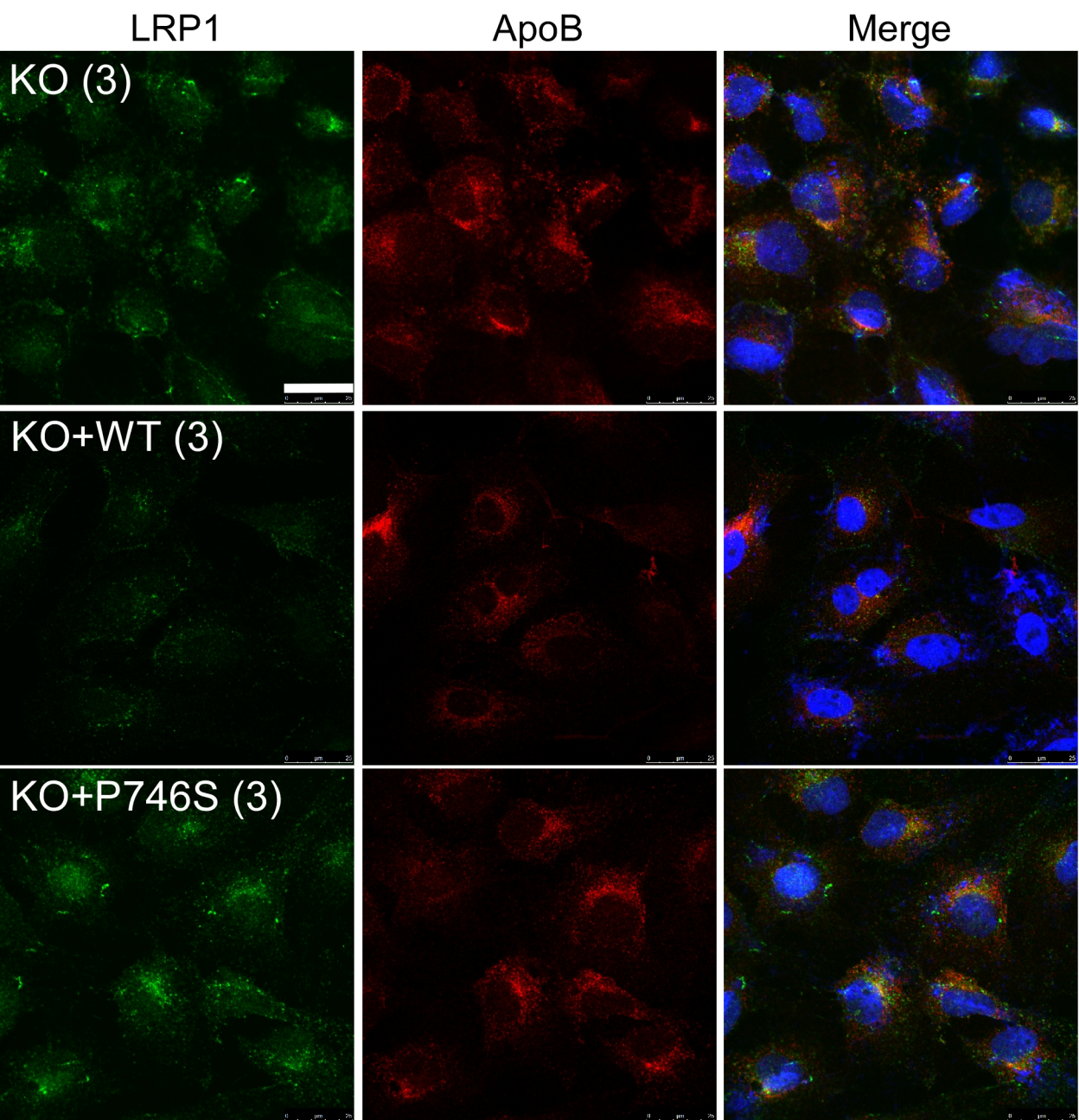


Figure S6

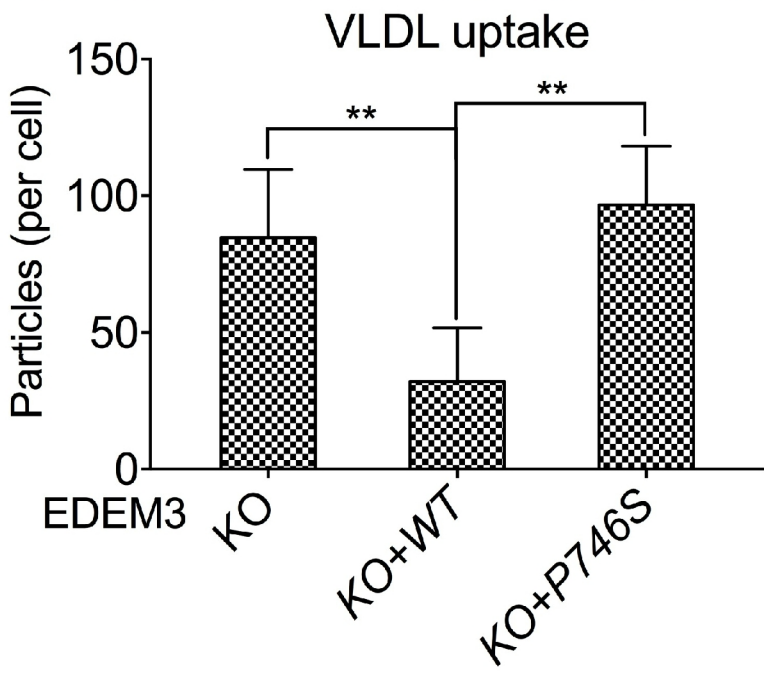
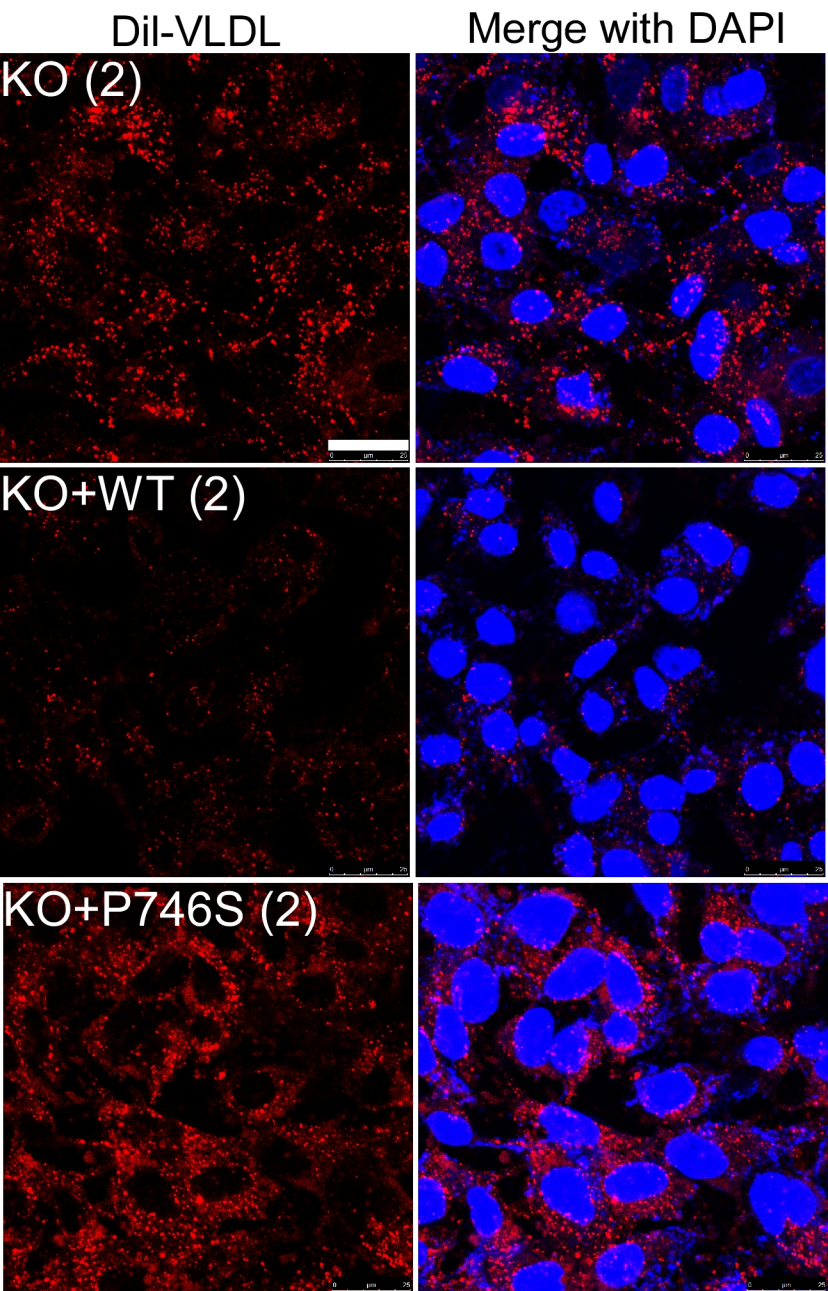
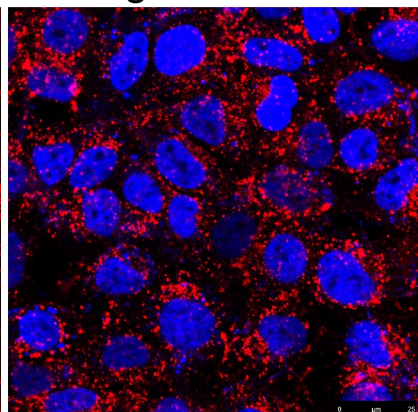
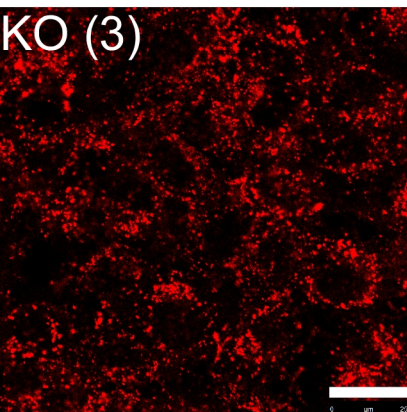


Figure S7

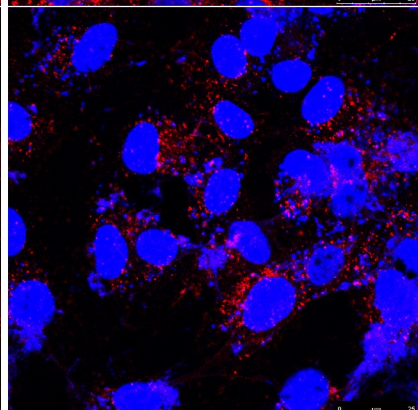
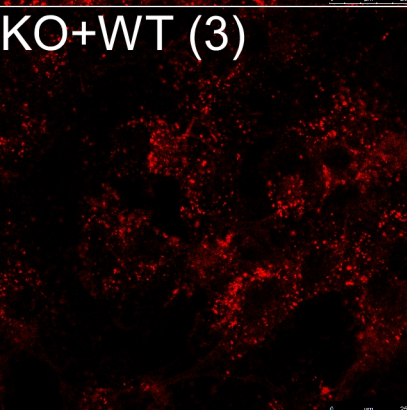
Dil-VLDL

Merge with DAPI

KO (3)



KO+WT (3)



KO+P746S (3)

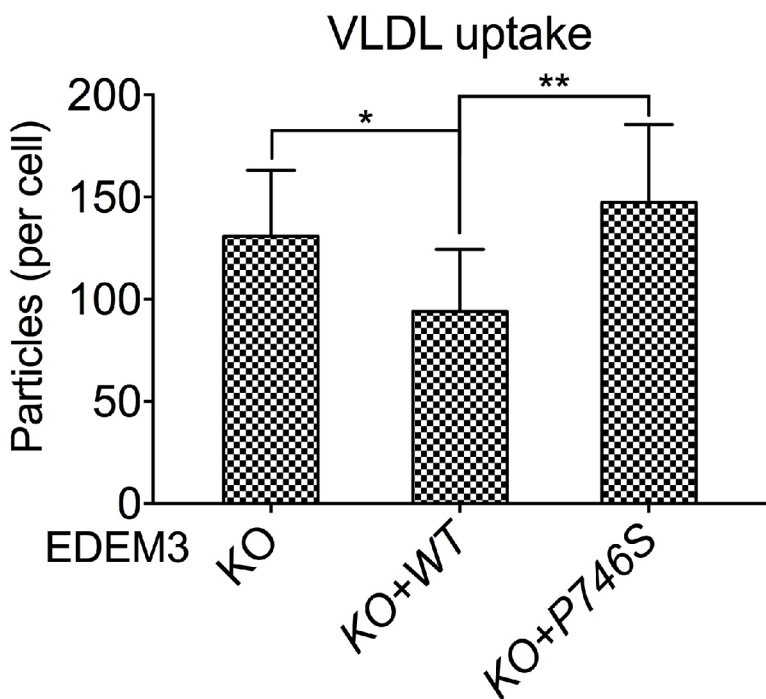
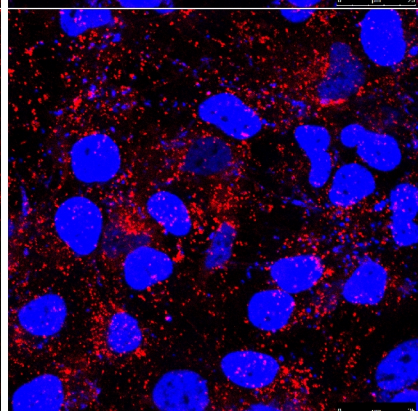
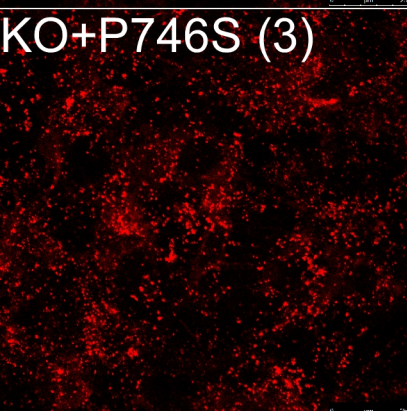
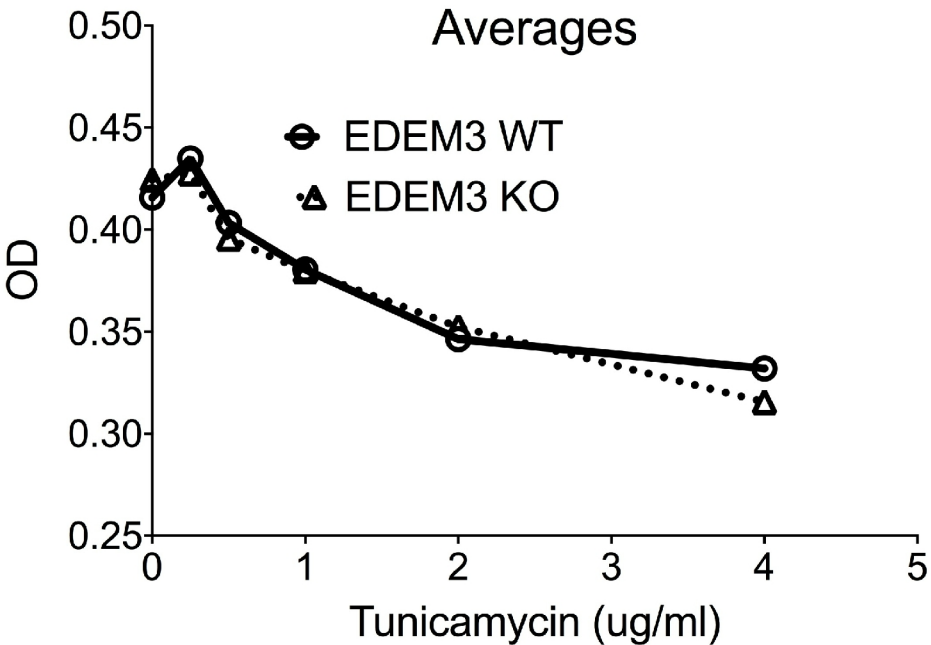


Figure S8



## Supplemental figure legends

**Figure S1. Related to Figure 1. Common variants near EDEM3 are not associated with blood TGs in the population.**  $-\log_{10}(p\text{-value})$  of the association between TG levels and variants near EDEM3 reported in Willer et al., 2013 is plotted on the y-axis against the variant position on the x-axis.

**Figure S2. Related to Figure 3. Deletion of EDEM3 gene did not affect Dil-LDL uptake.** Three individual EDEM3 scramble control (WT) and KO HepG2 (A) and Huh7 (B) clones were incubated with Dil-LDL. Tops, Representative images of the uptake assays from EDEM3 KO and control cells. Bottoms, Quantification of the uptake assays from three clones of the control cells (>100 cells) and KO cells (>560 cells). Cellular Dil-VLDL particle areas were quantified using ImageJ. The error bars represent SEM in the figure.  $p$  values (t-test) were calculated by comparing the KO cells with the control cells. N.S., not significant. Bar, 25  $\mu\text{m}$ .

**Figure S3. Related to Figure 3 and S2. Deletion of EDEM3 gene did not alter LDLR expression.** Extracts from three individual EDEM3 scramble control (WT), KO HepG2 (A) and Huh7 (B) clones were analyzed with Western blotting and probed with anti-LDLR and  $-\beta$ -actin antibodies. Western images were quantified with ImageJ. The error bars represent SEM in the figure.  $p$  values (t-test) were calculated by comparing the results from the KO cells with those from the control cells. N.S., not significant.

**Figure S4. Related to Figure 5-7. Complementary analysis of EDEM3 gene deletion in HepG2 cells with WT and P746S mutant EDEM3 on LRP1 expression.** Top, The control and complementary HepG2 cells as in Figure 7 were immunostained with antibodies against LRP1 and ApoB. The cells were analyzed under confocal microscope. Bottom, Image quantification of LRP1 and ApoB signal was carried out using ImageJ from 100-200 cells per clone. The error bars represent SEM in the figure.  $p$  values (t-test) were calculated by comparing the KO+WT cells with the KO or KO+P746S cells. \*,  $p < 0.05$ . ANOVA  $p$  value  $< 0.05$  for LRP1 expression;  $p$  value  $< 0.05$  for ApoB signal. Bar, 25  $\mu\text{m}$ .

**Figure S5. Related to Figure 5-7. Complementary analysis of EDEM3 gene deletion in Huh7 cells with WT and P746S mutant EDEM3 on LRP1 expression.** Similar analysis as in Figure S4 but for Huh7 cells (100-200 cells per clone).  $p$  values (t-test) were calculated by comparing the KO+WT cells with the KO or KO+P746S cells. The error bars represent SEM in the figure. \*,  $p < 0.05$ ; \*\*,  $p < 0.01$ ; \*\*\*,  $p < 0.001$ . ANOVA  $p$  value  $< 0.001$  for LRP1 expression;  $p$  value  $< 0.01$  for ApoB signal. Bar, 25  $\mu\text{m}$ .

**Figure S6. Related to Figure 7 and S4. Complementary analysis of EDEM3 gene deletion in HepG2 cells with WT and P746S mutant EDEM3 on VLDL uptake.** Top, The control and complementary HepG2 cells as in Figure 7 were used for the VLDL uptake assay as in Figure 3. The cells were analyzed under confocal microscope. Bottom, Image quantification of the uptake was carried out using ImageJ from 100-269 cells per clone. The error bars represent SEM in the figure.  $p$  values (t-test) were calculated by comparing the KO+WT cells with the KO or KO+P746S cells. \*\*,  $p < 0.01$ . ANOVA  $p$  value  $< 0.0001$ . Bar, 25  $\mu\text{m}$ .

**Figure S7. Related to Figure 7 and S5. Complementary analysis of EDEM3 gene deletion in Huh7 cells with WT and P746S mutant EDEM3 on VLDL uptake.** Similar analysis as in Figure S6 but for Huh7 cells (100-220 cells for each clone).  $p$  values (t-test) were calculated by comparing the KO+WT cells with the KO or KO+P746S cells. The error bars represent SEM in the figure. \*,  $p < 0.05$ ; \*\*,  $p < 0.01$ . ANOVA  $p$  value  $< 0.001$ . Bar, 25  $\mu\text{m}$ .

**Figure S8. Related to Figure 9. Deletion of EDEM3 gene did not change the response of the cells to ER stress.** The WT and KO HepG2 clones were incubated in media without or with increasing amount of tunicamycin as indicated. Viability of the cells was measured using alamarBlue reagent and absorbance was monitored at 570 nm.

Table S1. Related to Figure 1. EDEM3 missense mutations associated with lipid phenotypes

RSID	CHR:POS**	REF	ALT	Protein Change	Alternate Allele Frequency	Trait*	Sample Size	Beta***	SE	p-value
rs141657255	1:184663288	C	A	W903L	0.03%	TG	284295	0.0194	0.0803	0.8092
						LDL	274616	-0.0931	0.0809	0.2497
						HDL	295092	-0.0595	0.0806	0.4607
rs9425343	184663537	A	C	I820S	39.15%	TG	304422	0.0019	0.0027	0.4774
						LDL	294565	0.0070	0.0027	0.0108
						HDL	315135	-0.0010	0.0027	0.7183
<b>rs78444298</b>	<b>1:184672098</b>	<b>G</b>	<b>A</b>	<b>P746S</b>	<b>1.50%</b>	<b>TG</b>	<b>262076</b>	<b>-0.0502</b>	<b>0.0115</b>	<b>1.2x10<sup>-05</sup></b>
						LDL	253261	0.0005	0.0117	0.9645
						HDL	272904	0.0045	0.0112	0.6838
rs200489181	1:184681571	T	C	N511S	0.01%	TG	283685	0.0451	0.1403	0.7478
						LDL	273994	-0.0428	0.1404	0.7603
						HDL	294447	0.1643	0.1402	0.2413
rs139183949	1:184690424	G	A	T317I	0.01%	TG	284269	0.0697	0.1849	0.7062
						LDL	274520	-0.0814	0.1845	0.6592
						HDL	294971	-0.2787	0.1849	0.1317
rs202039206	1:184695486	C	T	R217Q	0.71%	TG	239249	-0.0109	0.0177	0.5387
						LDL	229888	-0.0295	0.0182	0.1051
						HDL	242531	-0.0023	0.0177	0.8952
rs201274616	1:184703729	T	C	R132G	0.02%	TG	274028	-0.0297	0.1040	0.7749
						LDL	264439	-0.0767	0.1063	0.4705
						HDL	284805	0.0101	0.1051	0.9236

\*TG was log transformed before analysis

\*\*Positions are on hg19

\*\*\*Beta is in standard deviation units

## **Transparent methods**

### **Cell culture, whole cell extracts, antibodies and Western blotting analysis.**

EDEM3 KO and WT control Huh7 and HepG2 cells were cultured in DMEM medium (Invitrogen) supplemented with 10% fetal bovine serum (FBS). Whole cell extracts were prepared with the lysis buffer containing 150 mM NaCl, 50 mM Tris (pH 7.5), 1% IGPAL-CA-630 (Sigma # I8896) and protease inhibitor cocktail (Roche). Western blotting analysis were performed using precast Mini-PROTEAN TGX SDS-PAGE (4-20%) (Bio-Rad). Blots were probed with anti-EDEM3 (Sigma, E0409) and  $\beta$ -actin (Santa Cruz, sc-47778) mouse monoclonal antibodies, and anti-LRP1 (Abcam, ab92544), anti-LDLR (Sigma, HPA013159), and -GAPDH (Cell Signaling, 3683S) rabbit antibodies.

### **EDEM3 gene deletion using CRISPR/Cas9 genome editing.**

EDEM3 KO cells were generated as previously described. Briefly, three single guide RNA (sgRNA) oligoes, 5'-GCCAGCGCGATGGAGACTAG-3', 5'-ATGGAGACTAGTGGCGGCGA-3', and 5'-CCGGCTTTCAACTACTACCAG-3' were designed to target exon 1 and 5 of human *EDEM3* gene and subcloned into lentiGuide-Puro vector. The vectors containing EDEM3 sgRNAs or a scramble control sgRNA (5'-GCACTACCAGAGCTAACTCA-3') together with accessory plasmids for lentivirus assembly were co-transfected into 293T cells for lentivirus production (Sanjana et al., 2014; Shalem et al., 2014). Packaged viruses were used to transduce the Cas9-expressing HepG2 and Huh7 cells for ~16 hrs. The transfected cells were treated with puromycin (5  $\mu$ g/ml) for five days. Subsequently, single cell clones were screened and the EDEM3 KO was confirmed with Western analysis with anti-EDEM3 and anti- $\beta$ -actin antibodies.

### **ApoB-100 secretion and measurement, and VLDL/LDL uptake assays.**

Time-course ApoB-100 secretion assays were carried out as previously described (Xu et al., 2018). Briefly, EDEM3 KO and control HepG2 and Huh7 cells (3 clones) were splitted and next day the cells were washed with serum-free media and incubated with serum-free medium. At various times media was taken for ApoB-100 measurement using ELISA kit (MABTECH) according to the manufacturer's instructions. The amount of ApoB-100 was normalized with cell numbers.

For VLDL/LDL uptake assays, EDEM3 KO and control HepG2 and Huh7 cells with, and the KO cells with WT/mutant EDEM3 complementation and relevant controls were incubated in serum-free medium (2 hrs) followed by incubation in serum-free medium containing Dil-VLDL and Dil-LDL (Stephan and Yurachek, 1993) (5  $\mu$ g/ml, Invitrogen) for 1 hr. The cells were then fixed and analyzed under confocal microscope as described below.

### **Confocal microscopy and image analyses.**

The cells from the above Dil-VLDL and Dil-LDL uptake assays, and WT and KO HepG2 and Huh7 cells without and with WT or P746S mutant EDEM3 complementation were fixed with a PBS buffer containing 3% paraformaldehyde (Santa Cruz, sc-281692) and 2% sucrose for 10 min. After washing, the cells from the uptake assays were processed for image collection under confocal microscope. The other cells were permeablized with Triton X-100 buffer (0.5% Triton X-100, 20 mM HEPES-KOH, pH 7.9, 50mM NaCl, 3mM MgCl<sub>2</sub>, 300 mM sucrose) (Xu et al., 2010). The cells were then blocked in PBG [PBS buffer containing 0.5% bovine serum albumin and 0.2% gelatin (Sigma G7765)] and incubated with anti-LRP1 and anti-ApoB monoclonal (Santa Cruz, sc-13538) antibodies and appropriate secondary antibodies. The coverslips were mounted in mounting media (Vector Laboratories, P36931). All the images were collected by scanning the slides with Leica SP5 AOBs Scanning Laser Confocal Microscope. The images were analyzed with ImageJ fiji. Constant thresholds were applied for all the images for the relevant series of experiments. Particle analysis was used to collect the cell particle number and size data.

### **Lentivirus preparation and complementation of EDEM3 KO with WT and P746S mutant EDEM3**

Human WT EDEM3 cDNA was purchased from Genescript (Clone ID OHu101917). The P746S mutation was generated using Quickchange site-directed mutagenesis (Agilent Technologies, 200519-5) according to the manufacturer's procedures. The cDNAs were cloned into the expressing vector FU-tetO-Gateway (Addgene, #43914) using Gateway Technology (Invitrogen) according to the manufacturer's procedures. The constructs without an insert or containing WT and mutant EDEM3 cDNAs were used for lentivirus production at the viral core of Boston Children's Hospital. Both the WT and mutant cDNA sequences were confirmed by DNA sequencing. The lentivirus particles were then used to incubate with EDEM3 KO HepG2 and Huh7 cells. Single cell clones were screened for the expression of WT and mutant EDEM3 using Western analysis with anti-EDEM3 antibody.

### **Adeno-associated virus (AAV) preparation and CRISPR/Cas9 KD of hepatic EDEM3 expression in mice**

A cell based in vitro system was used for screening the sgRNAs targeting mouse EDEM3 exon 1. Briefly, mouse EDEM3 sgRNAs were cloned into pX602 plasmid containing Cas9 from *Staphylococcus aureus* (SaCas9). A genomic fragment containing the target sites of EDEM3 sgRNAs were cloned into pCAG-EGXFP plasmids. The two plasmids were co-transfected into 293T cells. The EGFP fluorescence intensity in the transfected cells was monitored for the cleavage efficiency of the sgRNAs. A total of 25 EDEM3 sgRNAs were screened. The pX602 constructs containing the most efficient sgRNA (5'-CGGCTGCCGGGGCTGTGGGT-3') or a scramble control sgRNA (5'-TTTTTTGTTTTTTGTTTTTT-3') were used for AAV production at the Penn Vector Core. The AAV preparations (total droplet digital genome copy titer, 4.716E+12) were injected into WT mice (C57BL/6J, female, 12 weeks ) (Jackson Laboratory) followed by TG-rich high fat diet (Envigo, TD.06414). Blood samples were collected prior to the injection and weekly after the injection. The mice were sacrificed in about one month later. The liver samples were collected.

### **Cell surface fluorescein-labeled ConA staining and flow cytometry analysis**

EDEM3 KO and control HepG2 cells were blocked with BSA in PBS with 5% FBS and 2 mM sodium azide on ice for 20 min. The cells were then pelleted and resuspended in PBS with fluorescein-labeled ConA (10 ug/ml) (Vector laboratories, FL1001) on ice for 30 mins. The cells were pelleted again and resuspended 250 ul PBS. About 2.5 ml cold paraformaldehyde (1%) was added in dropwise to the cell suspension and incubated on ice for 15 min. The cells were washed twice with cold PBS. The cell pellet was resuspended in 250 ul cold PBS and 1 ml cold 70% ethanol was added in dropwise. The suspension was incubated on ice for 20 min and pelleted. The pellet was resuspended in 500 ul PBS and analyzed with flow cytometer (Becton Dickinson) at the HSCI-CRM Flow Cytometry Core Facility of MGH. The data were analyzed with FlowJo software.

### **Tunicamycin stress test**

EDEM3 KO and control HepG2 cells were treated with increasing amount of tunicamycin (Sigma-Aldrich) for 4 days (Graham et al., 2016). Cell viability was then analyzed with alamarBlue reagent (Thermo Fisher, DAL1025) according to the manufacturer's protocol and absorbance was monitored at 570 nm.

### **Plasma TG measurement and Western analysis of liver extracts**

The mouse plasma TG was measured with triglyceride colorimetric assay kit (Cayman, 10010303) according to the manufacturer's protocol. Liver lysates were prepared in 1XTBS containing 1% NP-40 and 0.1% sodium doxycholate with the protease inhibitor cocktail (Roche). The liver lysate (~50 ug total protein) was used for Western analysis with anti-EDEM3 and -LRP1 antibodies. All quantitation was normalized to the endogenous mouse GAPDH.

### **Total RNA extraction and RNA-seq analysis**

Total RNA from EDEM3 WT and KO HepG2 cells was extracted using RNeasy Mini Kit (Qiagen) according to the manufacturer's procedures. RNA-seq analysis was performed at the Translational Genomics Core of Partners HealthCare.

### **Total cell lipid extract preparation and metabolite mass spectrometry analysis.**

Preparation and metabolomics analysis of total cell lipid extracts from *EDEM3* KO and scramble control HepG2 cells were carried out as previously described (Mascanfroni et al., 2015). The blood lipid metabolite data of the individuals carrying SNP rs78444298 (P746S) were obtained from FHS 1000G GWAS cohorts as previously described.

### **Statistic analysis.**

Statistic analyses for functional assays were performed using Prism 7 (GraphPad) with the student's t-test or one way analysis of variance (ANOVA). Detailed group comparisons were described in individual figure legends. *p* values of  $\leq 0.05$  were considered to be statistically significant (\*,  $p < 0.05$ ; \*\*,  $p < 0.01$ ; \*\*\*,  $p < 0.001$ ).

### **Key resources table**

<b>Reagents or Resources</b>	<b>Source</b>	<b>Identifier</b>
<b>Antibodies</b>		
Mouse monoclonal against EDEM3	Sigma-Aldrich	E0409
Mouse monoclonal against $\beta$ -actin	Santa Cruz	sc-47778
Rabbit monoclonal against LRP1	Abcam	ab92544
Rabbit monoclonal against GAPDH	Cell Signaling	3683S
<b>Chemicals, reagents</b>		
Protease inhibitor cocktail	Roche	05892791001
IGPAL-CA-630	Sigma-Aldrich	I8896
Tris buffered saline (10X, pH 7.4)	Boston BioProducts	BM-300
Doxycycline	Sigma-Aldrich	D1822
Tunicamycin	Sigma-Aldrich	T7765
FBS (heat inactivated)	SAFC	12306C
Puromycin	Sigma-Aldrich	SBR00017
NP-40 substitute	Sigma-Aldrich	I8896
Paraformaldehyde (4%)	Santa Cruz	Sc-281692
Sodium chloride (5M)	Boston BioProducts	BM-244
Tris-HCl buffer (1M, pH 7.5)	Boston BioProducts	BM-315
Dil-LDL	Alfa Aesar	BT-904
Dil-VLDL	Alfa Aesar	BT-922
Fluorescein-labeled ConA	Vector laboratories	FL1001
Isopropanol (for metabolomics)	Fisher Chemical	BP2632-4
Methanol (for metabolomics)	Fisher Chemical	A456-4
<b>sCommercial assays</b>		
ApoB ELISA kit	MABTECH	3715-1H-6
Triglyceride colorimetric assay kit	Cayman	10010303
RNeasy Mini Kit	Qiagen	74104

alamarBlue reagent	Fisher Scientific	DAL1025
Quickchange site-directed mutagenesis	Agilent Technologies	200519-5
Gateway BP clonase II enzyme mix	Introgen	11789-020
Gateway LR clonase II enzyme mix	Introgen	11791-020
<b>Vectors, cDNA</b>		
WT EDEM3 cDNA	Genescript	OHu101917
lentiGuide-Puro	addgene	52963
FU-tetO-Gateway	addgene	43914
pCAG-EGXXFP	addgene	50716
pX602	addgene	61593
<b>Core facility services</b>		
WT and P746S EDEM3	Boston Children's Hospital viral core	Custom
Lentivirus preparation		
EDEM3 CRISPR AAV preparation	Penn Vector Core	Custom
Flow cytometry	MGH HSCI-CRM Flow Cytometry Core Facility	
RNA-seq analysis	Partners HealthCare Translational Genomics Core	
Metabolomics analysis	Broad Institute metabolomics platform	
<b>Mouse strain and diet</b>		
C57BL/6J	The Jackson Lab	000664
High fat diet	Envigo	TD.06414
<b>Software and quantification</b>		
GraphPad Prism 7	GraphPad software	<a href="http://graphpad.com">http://graphpad.com</a>
ImageJ software	ImageJ	<a href="http://imageJ.net">http://imageJ.net</a>